Comparing Wind-Driven Motion at LHO's Corner and End Stations Between O3a and O3b

LIGO-T2100269

February 3, 2021

Drew Gao, Brian Lantz

Abstract

Prior to O3b, wind-driven tilt coupling in the 30-100mHz bands of motion at the end stations significantly hindered the performance of the Hanford interferometer. However, at the start of O3b (November/December 2019) wind fences were installed at the end stations in an attempt to mitigate the problems associated with high winds. We see that the fences significantly reduce the tilt at the end stations. Comparing the effects of wind on the corner station and the two end stations following the installation of the wind fence, we can see that the effect of wind on the end stations has been reduced to the extent that high winds now have a greater impact on the corner station than either end station.

1. Introduction

LIGO's Hanford site has historically experienced strong winds which induce significant amounts of rotation at the end stations at frequencies <1 Hz. Due to tilt-horizontal coupling of the STS-2 sensors, high winds (>6 m/s) often result in unwanted signals in the seismic isolation systems, potentially leading to lock loss and other performance issues. Prior to the start of O2, Beam Rotation Sensors (BRS) were installed to subtract out the effects of tilt coupling on the STS-2 sensors [VEN18]. However the BRS tilt subtraction has a practical limit of a 10 factor reduction of the tilt signal which is measured by the STS-2 as horizontal motion, and high winds still caused a notable decrease in the performance of the interferometer. Thus, in the commissioning break between O3a and O3b, wind fences were installed to the southwest of both end stations with the intention of further reducing the effects of wind. These fences were completed shortly after the start of O3b around December 10th 2019. Pictures of the completed fences are included below.

Figure 1.1: End-X Wind Fence

Figure 1.2: End-Y Wind Fence

This paper provides a few different perspectives on the efficacy of the wind fences. In Section 3 we attempt to establish distinct relationships between tilt (i.e. BRS data) and wind speed during O3a and O3b. In Section 4 we do the same but with ground motion (i.e. raw STS-2 and tilt subtracted STS-2 data). Section 5 attempts to evaluate any change in the spread of building tilts, and raises questions for additional study. Section 6 looks at ground motion at the end stations relative to the corner station, and Section 7 looks at the duty cycle of the interferometer.

2. Notes on Data

In [GAO21], I discuss identifying characteristics of various sources of 30-100 mHz BLRMS motion. Since this paper aims to identify trends in motion caused by wind, unless explained otherwise all data discussed henceforth will isolate motion that is primarily wind-driven. Particularly, most problematic anthropogenic motion was removed by removing data from 7 a.m. PST to 1 p.m. PST on Tuesdays since these are the standard maintenance times during which anthropogenic noise can be observed in the 30-100 mHz bands. Earthquake-driven motion was also removed by removing data points for which the ITMY z-axis 30-100 mHz BLRMS motion was greater than 80 nm/s. To ensure proper attention was given to winds which have a noticeable effect on seismic isolation performance.

The majority of this study compares data from O3b following the completion of the fence (10 December 2019 – March 27 2020) and an equal duration period in O3a (1 April 2019 – 18 July 2019). Although the results of this paper are drawn from data taken during observing runs, only the results of Section 7 actually depend on the operational status of the interferometer. Thus future studies conducting similar analysis can use data from any period when SEI and PEM sensors were functioning as intended.

All data was acquired from the LIGO data grid with help from Jim Warner. Data files as well as code for plots can be found within the DCC entry for this paper. Note that due to a wiring error fixed in August of 2019, data from the ITMY sensor was recorded by the HAM2 channels. Any data labeled with HAM2 prior to August 6, 2019 is labeled based on the name of the channel in the data grid but actually corresponds to data from the ITMY sensor.

2.1 Note on Fence Placement and Wind Direction

Figures 2.1 and 2.2 show the wind fences at End-X and End-Y respectively. The fences were installed only on the southwest side of each end station since 10 years of wind data collected at a nearby (20 mi away) airport in Pasco, WA, indicated that high speed winds came from that direction a majority of the time [LAN18]. Due to topographical limitations, the End-X fence (Fig. 3Fig. 3) is straight while the End-Y fence (Fig. 4Fig. 4) is curved. Although the initial design of the End-Y fence had it shaped like a circular arc, the north end of the completed fence curves towards the building more so than the south end.

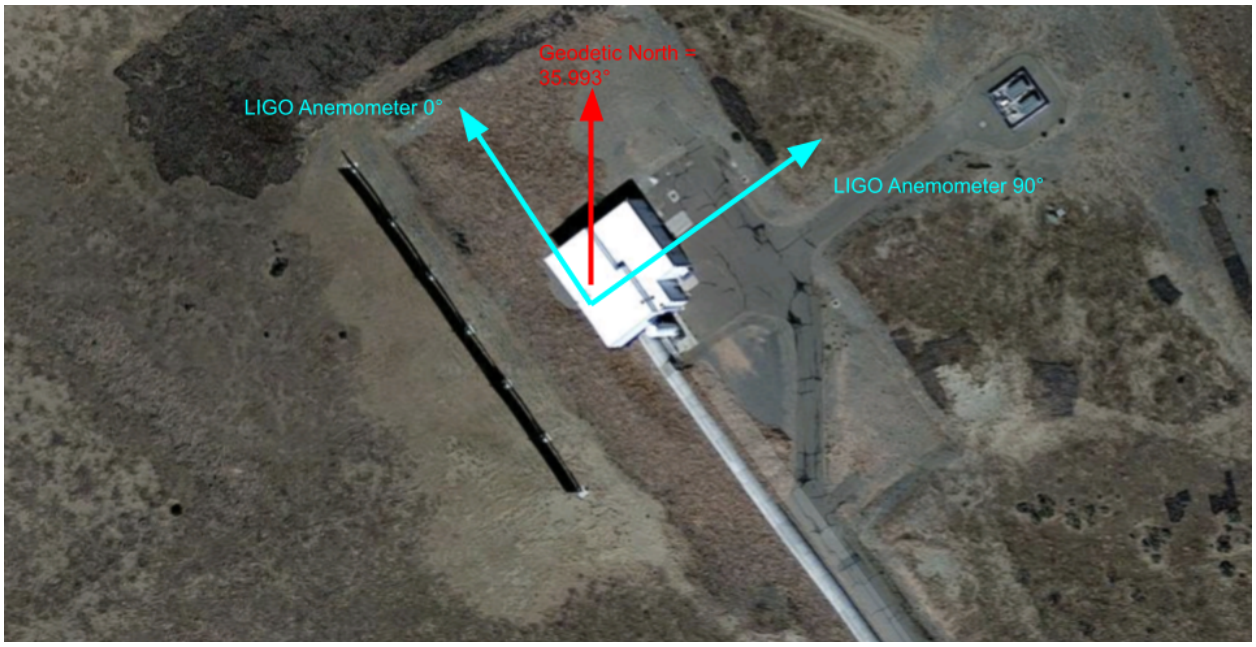

Figure 2.1: End-X Fence, Satellite View

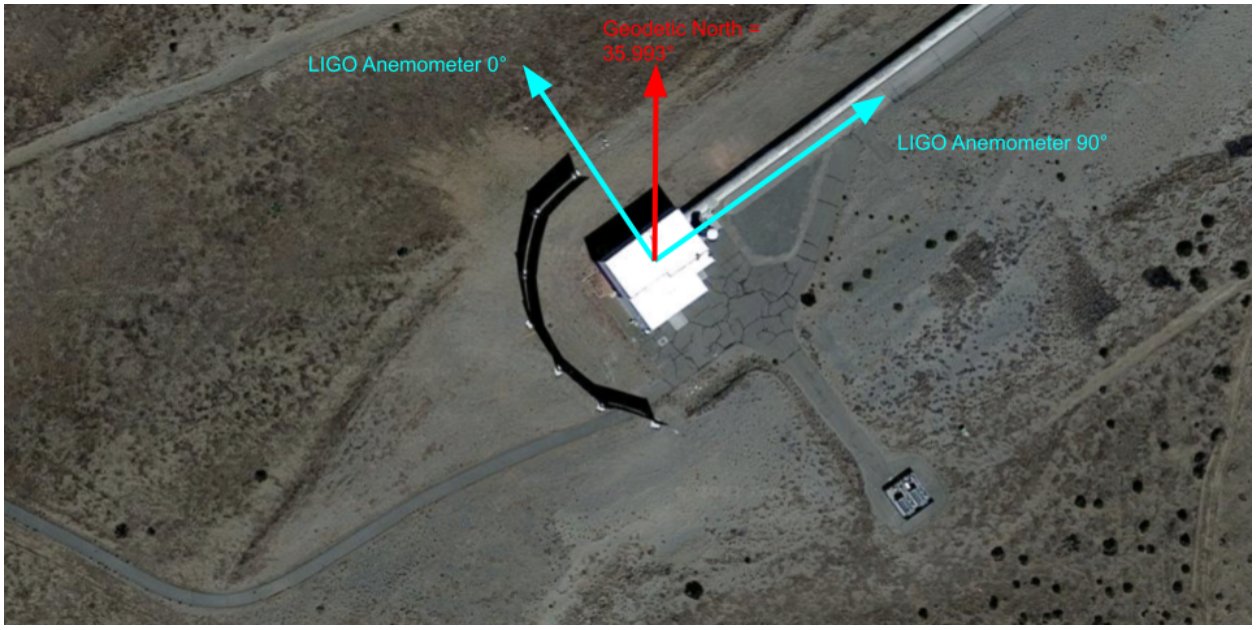

Figure 2.2: End-Y Fence, Satellite View

To confirm that the distribution of wind direction observed at Pasco airport matches that of LHO, Fig. 2.3 shows wind roses generated from wind speed and directions as measured by anemometers on top of the

corner station and End-X during O3a and O3b.[1] During O3b we see the expected dominance of high speed wind coming from the south-west directions (bottom right quadrant of plot). Particularly we see that at End-X, for wind speeds >6 m/s, which this study focuses on, the wind blows from the protected southwest direction about 85% of the time. However, during O3a wind faster than 6 m/s only blew from the south-west direction about 34% of the time compared to about 58% of the time which it blew from the northwest direction. Some possible sources of this deviation from the distribution of wind at Pasco airport could be the local topography influencing wind direction, the end station building influencing the wind direction measured on the roof, or simply natural variance in wind direction. However more work will need to be done to determine the cause of this deviation and to examine whether extra wind protection is needed to the north-west of the end stations as well.

1 Data from end Y was not shown as the end Y anemometer tends to get stuck and does not accurately measure wind direction

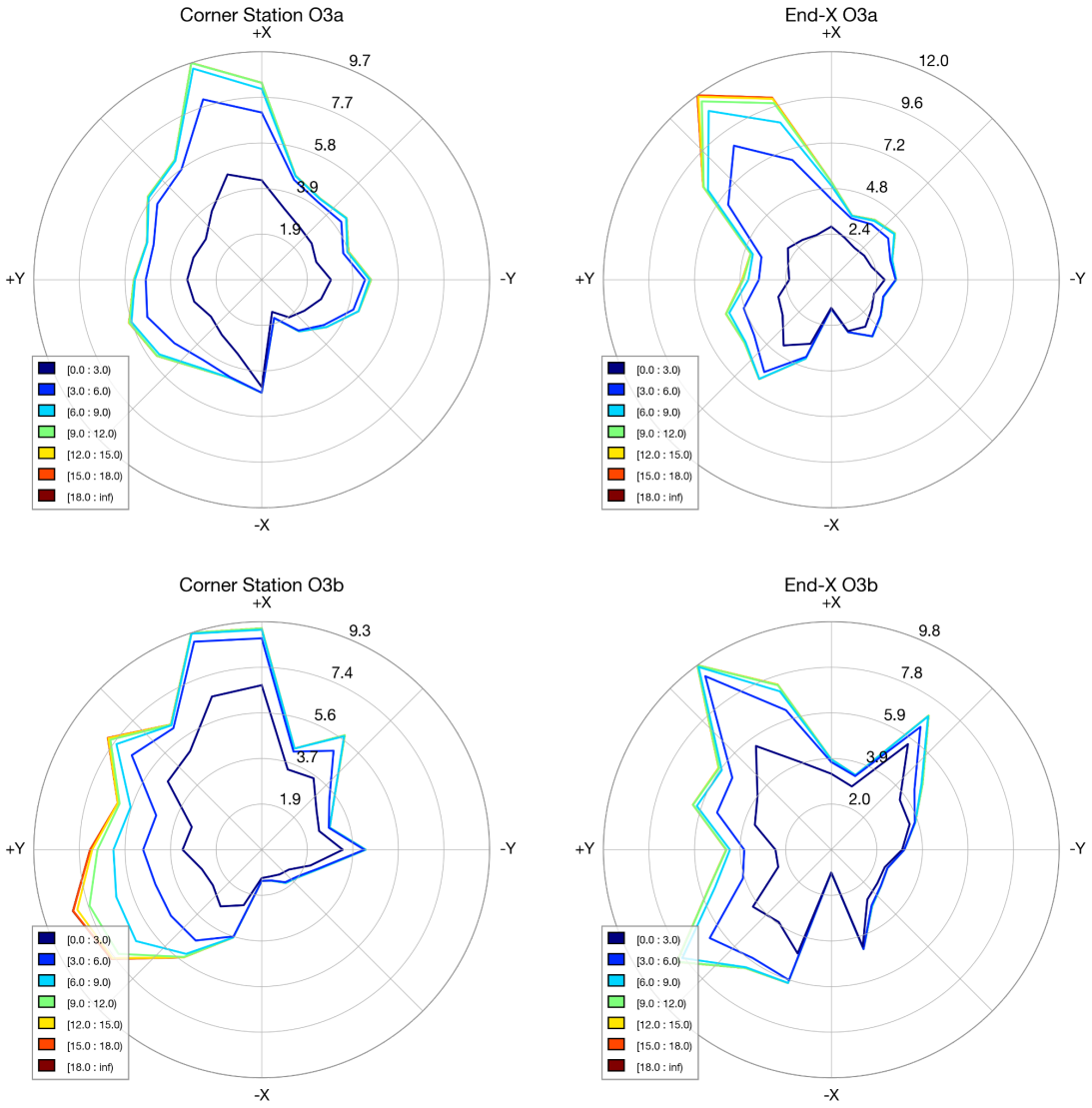

Figure 2.3a: Wind Roses for O3a and O3b, Corner Station and End-X. These show the direction the wind is coming from for a given speed range, oriented with the arm direction. The radius is measured in percentage of time

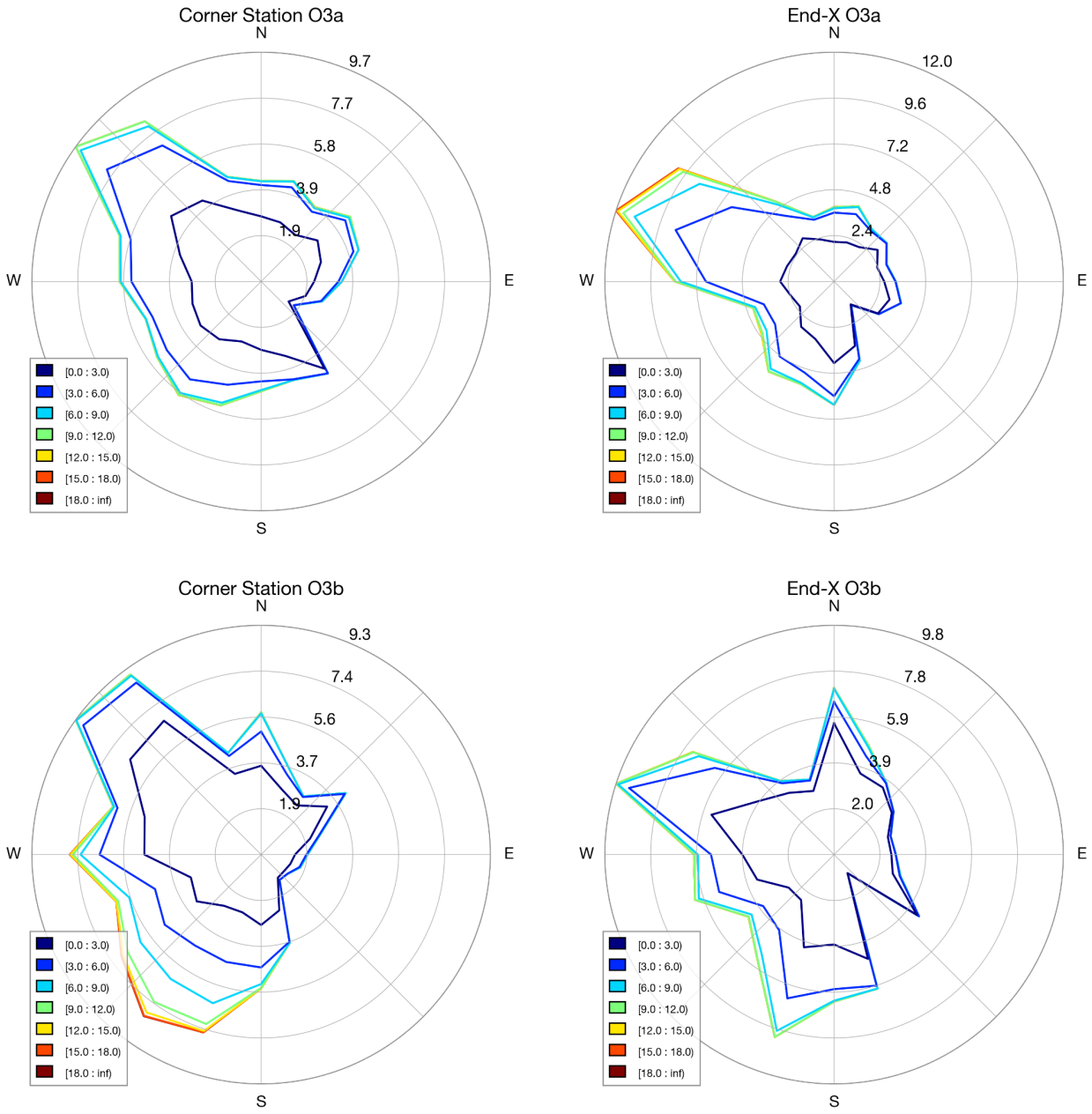

Figure 2.3b: Wind Roses re-oriented to the cardinal directions. **2.2 Note on Use of Corner Station Anemometers**

Since the primary PEM anemometers are located on top of each building, the sensors at the end stations fall downstream of the wind fence for wind blowing from the southwest direction. Thus in order to accurately compare wind speeds during O3a and O3b we need to use an anemometer unaffected by the wind fences. Due to the lack of a true free stream anemometer, the only reliable anemometer unaffected by the fences is the one on the corner station. Although anemometers do exist on the mid stations, these experience problems in reliability due to lack of regular maintenance. The use of the Corner Station wind data to evaluate motion at both End-X and End-Y also allows for more direct comparisons to be made between the motion at the end stations, for instance when comparing motion during times when wind speeds are >6 m/s, using the same anemometer when considering both end stations ensures that we are looking at identical time ranges for both end stations.

There is also an anemometer is located on the ground about 39 feet south-west of the End-X wind fence [ALOG54680], due to its near fence location and the lack of a similar sensor at End-Y, this sensor is only used to evaluate motion at End-X when winds blow from the southwest.

3. Effect of Wind Fence on Tilt

The primary purpose of the wind fences at End X and End-Y are to reduce the wind speed and thereby reduce the tilt. Previous computational fluid dynamic modeling work indicated that the fence would result in an ~ 50% reduction in wind speed whence we obtain a ~75% reduction in tilt [HOF19]. The following data indicates that while we do see a significant reduction in tilt during times when the wind blows in a direction which gets protection from the fence, this reduction is not quite as large as predicted by previous models. We also note some unexpected observations and propose some potential explanations.

3.1 Tilt at End-X vs Wind Speed

We have a number of anemometers which can be used to approximate the free stream wind speed at End-X each with their own drawbacks and benefits. Most important to us are the PEM-EX, PEM-CS located on top of the end station and the corner station respectively, as well as the anemometer located 39 feet southwest of the wind fence elevated 10ft above the ground (henceforth referred to as EX Ground). The PEM-EX anemometer comes with the drawback that its readings are affected by the wind fence for wind coming from the +Y direction. The PEM-CS anemometer, although unaffected by the fence, comes with the drawback of being 4km away from the actual end station. The EX ground anemometer, while unaffected by the fence for wind coming from the +Y direction, is affected by the fence for wind coming from the -Y direction.

3.1.1 Tilt at End-X vs Wind Speed Measured Upstream of Fence

Since our primary concern is wind coming from the +Y direction, this leaves the EX ground anemometer as the best choice for an anemometer for us to compare tilt to. A plot showing RY tilt as a function of wind speed (regardless of direction) is included below (Fig. 7). In this plot we can see significant reductions in tilt relative to wind speed across the entire range of wind speeds, however the improvement is especially noticeable for winds >6 m/s. For winds blowing at about 10 m/s we see a ~3 factor improvement in tilt following fence installation.

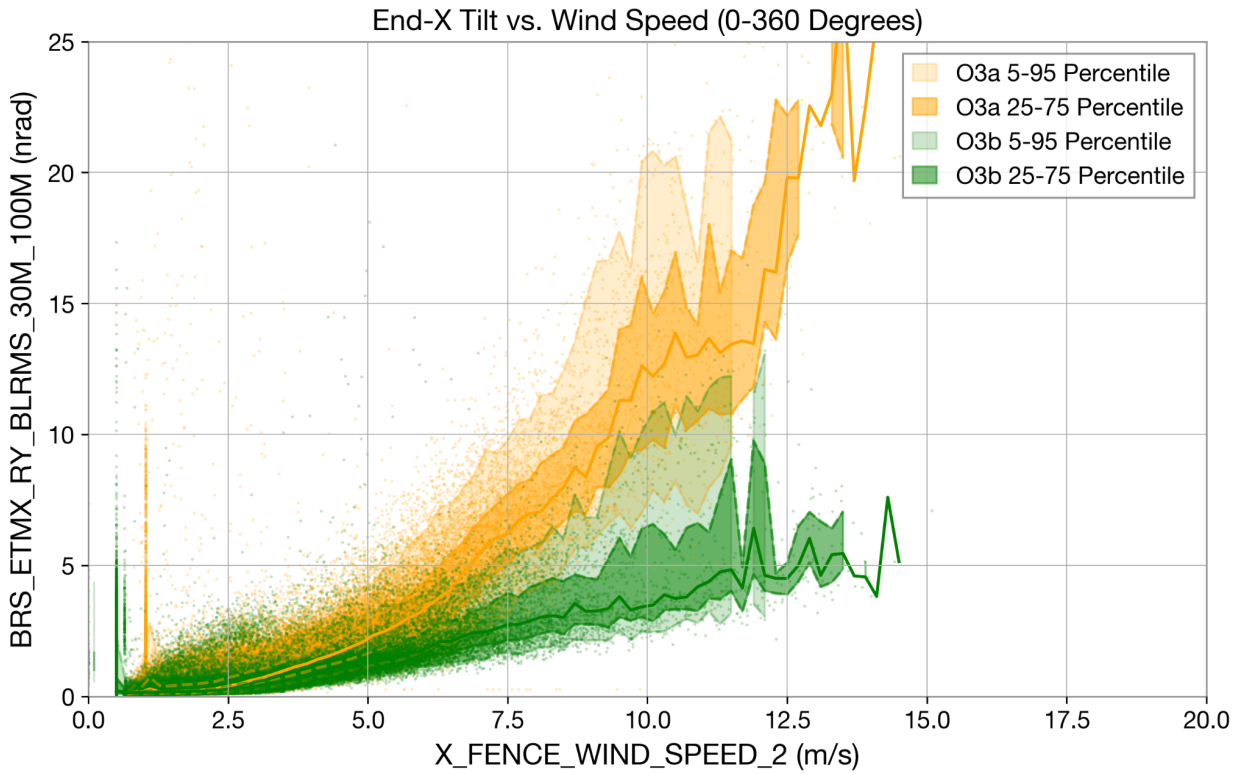

Figure 3.1: Tilt at End-X vs Wind Speed Measured on Ground: Orange and green areas show middle 90 and 50 percent of data from O3a and O3b respectively

To emphasize the effects of the fence as well as focusing on the direction of most concern to us (wind from the +Y) we focus on wind coming from the +Y direction in Fig. 8. We see a similar trend with the improvement being most noticeable for wind speeds >6 m/s. Due to a lack of wind > 8 m/s during O3a it is difficult to empirically evaluate the performance of the wind fence across the full range of wind speeds using this method.

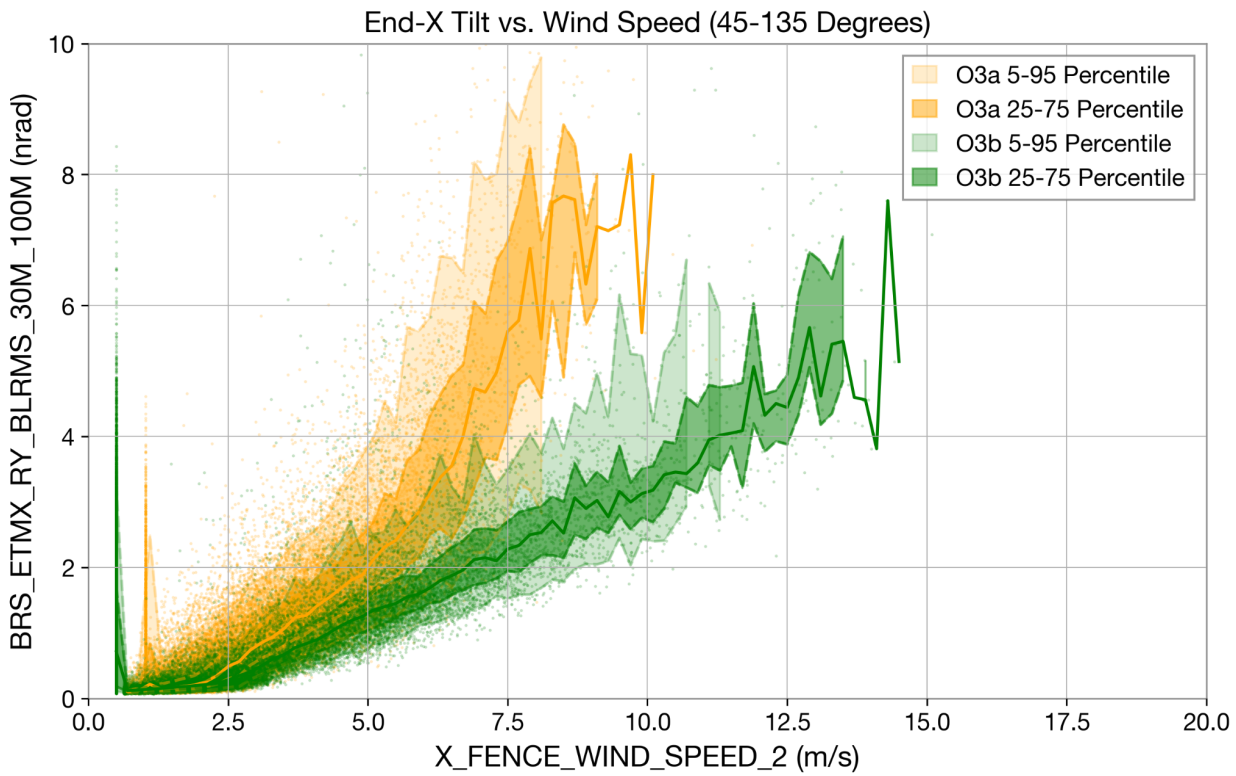

Figure 3.2: Tilt at End-X vs wind speed measured at Corner Station for wind blowing from the -Y direction: Orange and green areas show middle 90 and 50 percent of data from O3a and O3b respectively

Fig. 9 focuses on the second most problematic wind direction, wind coming from the +X direction. For these winds we see only a slight improvement between O3a and O3b. This slight improvement was likely a result of other improvements made during this time and not due to the fence as the placement of this fence allows wind from the +X direction to reach the end station unimpeded. Some wind coming from the -Y direction would also pass through the fence before reaching the anemometer causing wind speed readings which are lower than the actual wind speed.

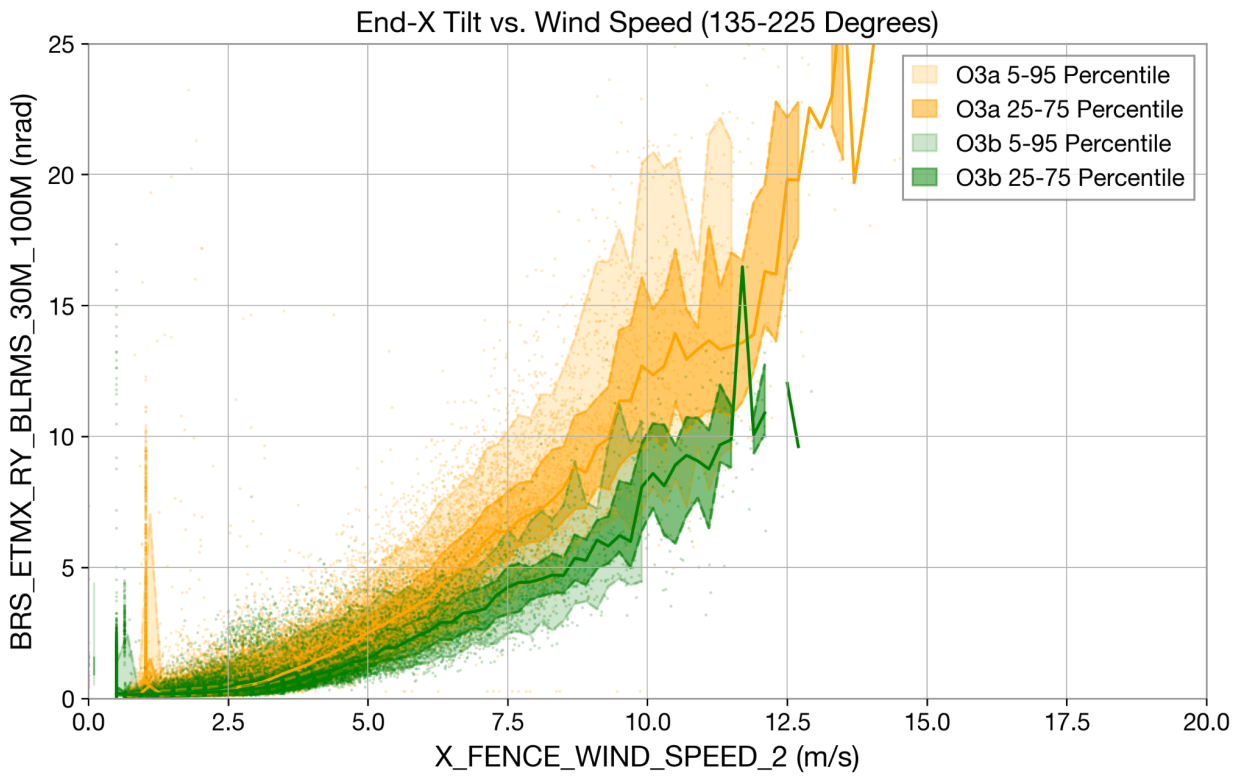

Figure 3.3: Tilt at End-X vs wind speed measured at Corner Station for wind blowing from the -X direction: Orange and green areas show middle 90 and 50 percent of data from O3a and O3b respectively

3.1.2 Tilt at End-X vs Wind Speed Measured on Top of End-X

As previously noted the wind fence also reduces the wind speed as measured from the top of End-X, which may obscure the true relationship between wind and tilt. Comparing the tilt at End-X with the wind speed measured on the roof of End-X for all directions, we see that there is a very slight reduction in tilt relative to the wind speed as measured on the roof of End-X for wind speeds greater than about 7.5 m/s. This can be seen in Figure 3.4. Even looking at only wind coming from the protected -Y direction in Figure 3.5 we see minimal if any statistically significant difference between the amounts of tilt during O3a and O3b. When looking at wind from the -X direction in Figure 3.6, we once again see very little difference in tilt between O3a and O3b. However we can notice that the magnitude of the tilt relative to wind speed is greater when the wind is coming from the -X direction than the -Y. Thus the reduction in tilt between O3a and O3b we see in Figure 3.4 is likely a consequence of a greater proportion of and higher speed wind coming from the -X direction during O3a than O3b.

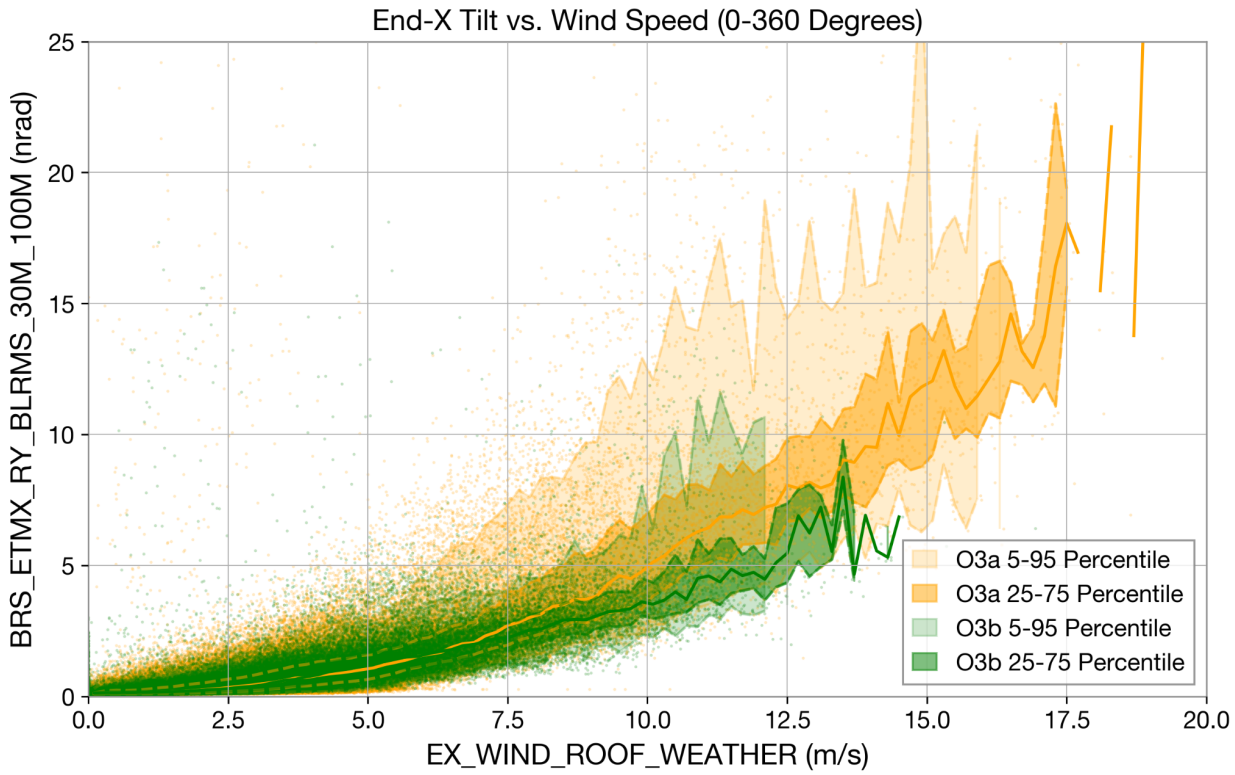

Figure 3.4: Tilt at End-X vs wind speed measured at End-X: Orange and green areas show middle 90 and 50 percent of data from O3a and O3b respectively

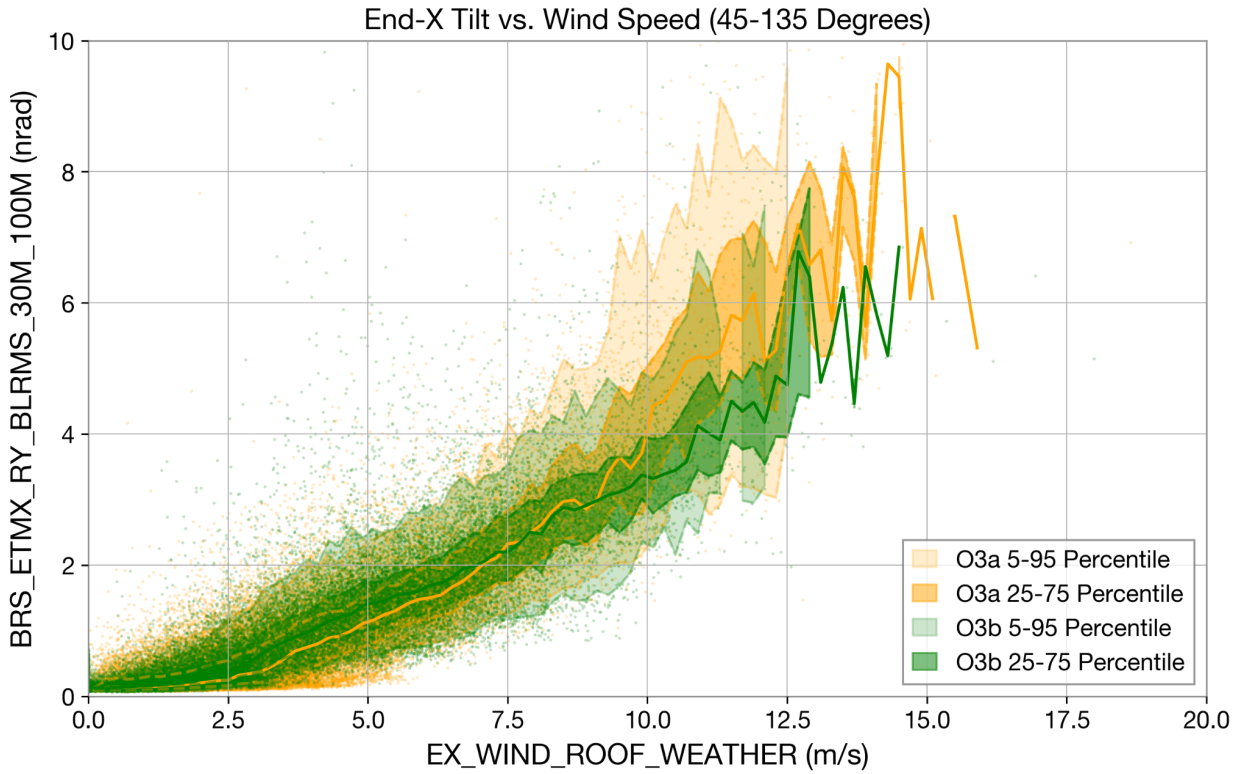

Figure 3.5: Tilt at End-X vs wind speed measured at End-X for wind blowing from the -Y direction: Orange and green areas show middle 90 and 50 percent of data from O3a and O3b respectively

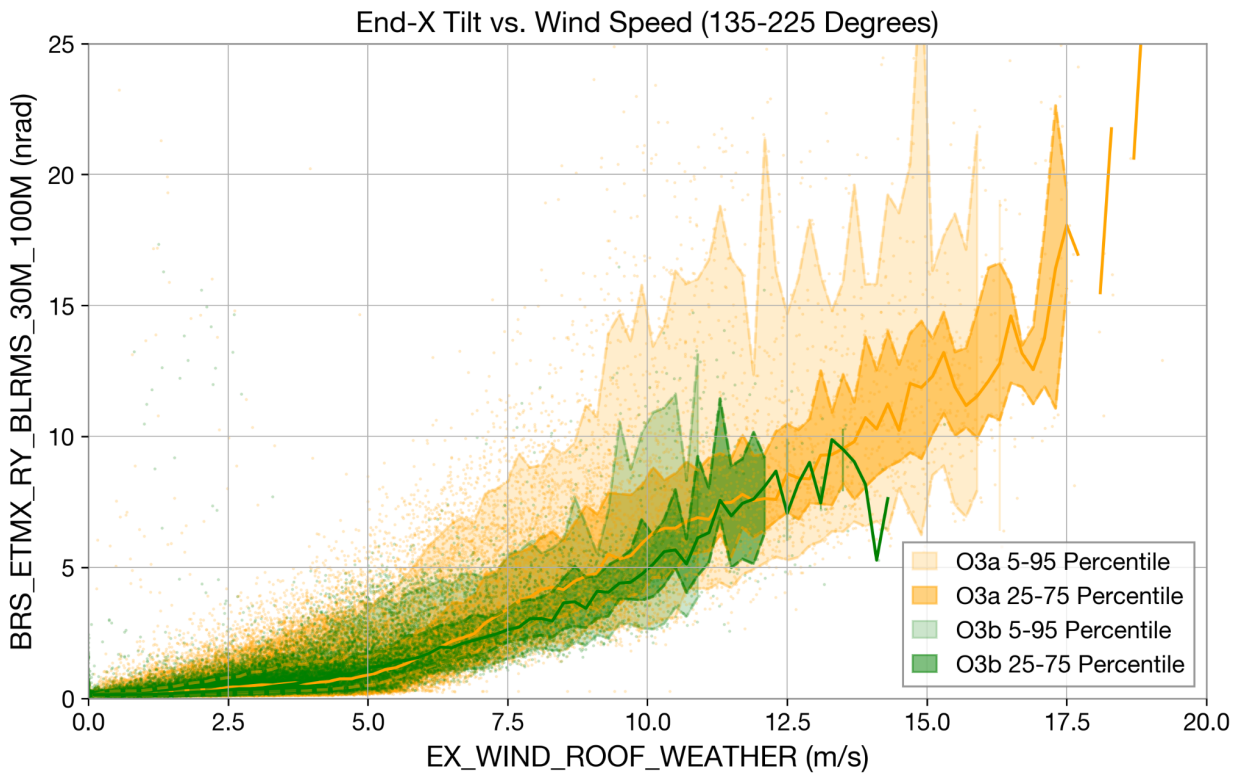

Figure 3.6: Tilt at End-X vs wind speed measured at End-X for wind blowing from the -X direction: Orange and green areas show middle 90 and 50 percent of data from O3a and O3b respectively

In Figures 3.4, 3.5, and 3.6, we see that there is little change between the building tilt and the wind speed as measured at the building top. The most likely explanation is that the wind fence reduces the wind speed measured on the rooftop. Since the anemometer is only elevated about 6 feet above the building, the wind measured by this anemometer is likely to be wind which has flowed into and over the bluff body of the end station exterior. Thus a reduction in the speed of wind hitting the side of the building (such as what we would expect from the wind fence) also results in a reduction in the wind speed measured by the rooftop PEM anemometer. This hypothesis is supported by Fig. 2.3 as we can see that despite wind speed generally being greater at End-X than at the Corner Station during O3a, wind speeds measured at End-X during O3b tended to be lower than wind speeds measured at the Corner Station during the same period, as well as by Figure 3.7 which explicitly shows the change in relationship between End-X rooftop wind measurements and wind measurements on the ground, upstream of the fence.

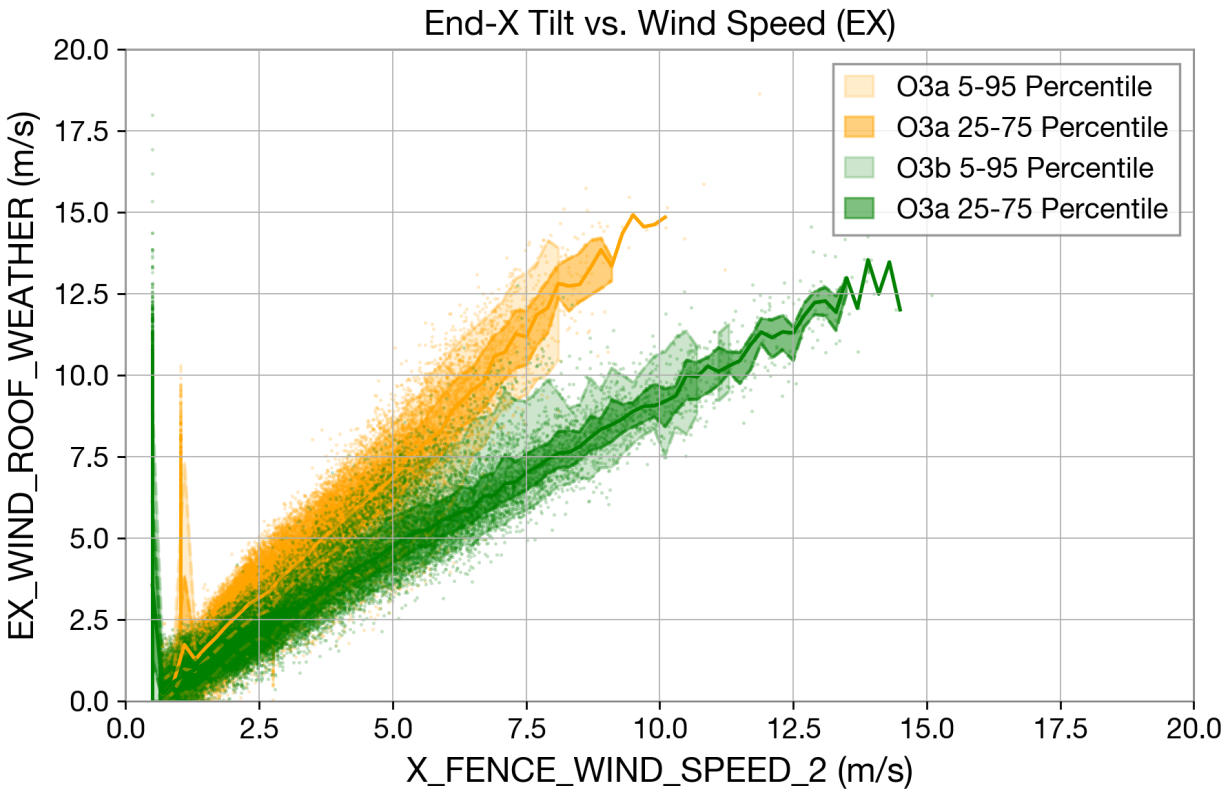

Figure 3.7: Wind speed measured on top of End-X vs wind speed measured on ground: Orange and green areas show middle 90 and 50 percent of data from O3a and O3b respectively

3.1.3 Tilt at End-X vs Wind Speed Measured At Corner Station

Here we replot results from 3.1.1 and 3.1.2 using wind speeds from the corner station. Although the distance between the Corner Station and End-X is likely to introduce some error to these results, comparing End-X tilts with the Corner Station anemometer allows us to make a more direct comparison with End-Y results. We see noticeable differences in the amount of tilt for a given wind speed between O3a (ie no fence) and O3b (fence protected) starting at around 5 m/s. This difference in the effect of wind on tilt at the X end station between O3a and O3b increases steadily until ~10 m/s where we see the largest benefit derived from the fence.

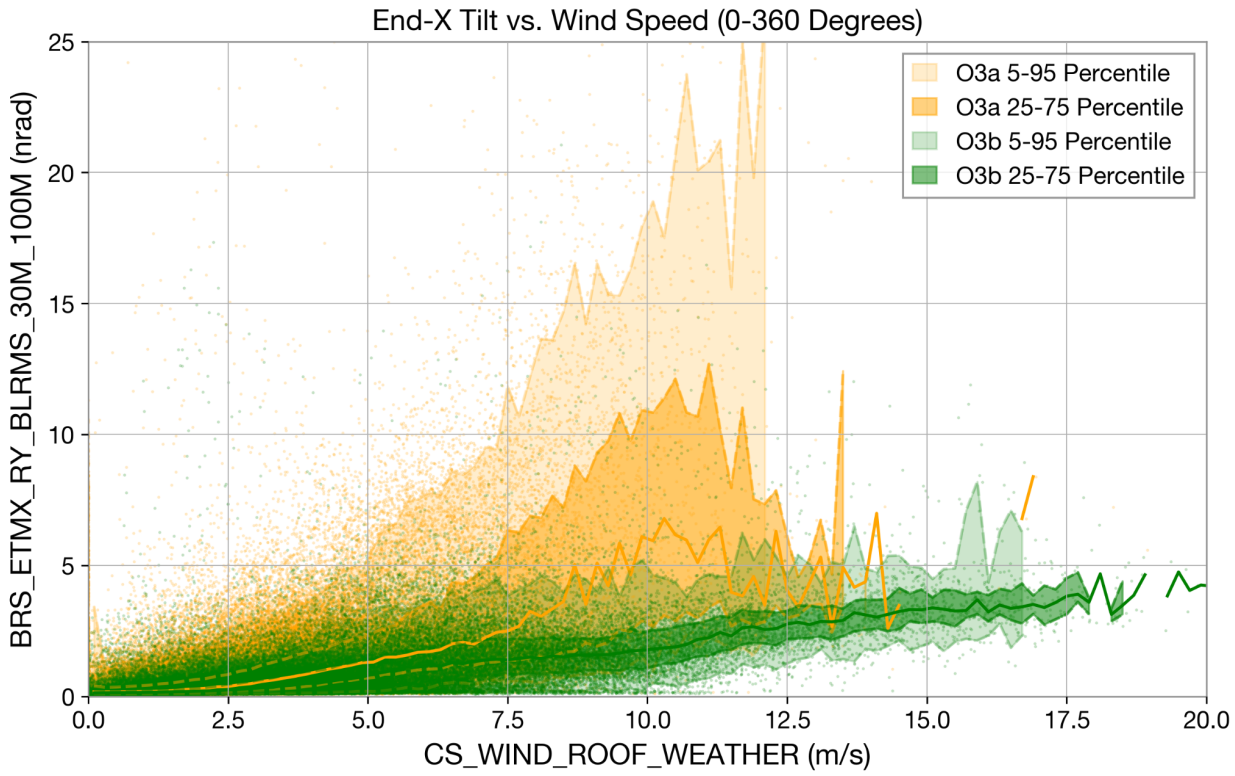

Figure 3.8: Tilt at End-X vs wind speed measured at Corner Station direction: Orange and green areas show middle 90 and 50 percent of data from O3a and O3b respectively

Interestingly, looking only at wind coming from the +Y direction using wind speed and direction measures from the corner station we see only a slight improvement in O3b (Fig. 3.9). However, looking at wind coming from the +X direction using wind speed and direction measures from the corner station results in a large difference which was not previously observed when using anemometers closer to End-X (Fig 3.10). Since the corner station is located 4km away from the end station it is possible that these results are influenced by the unreliability of using the corner station anemometer as a proxy for the End-X free stream wind speed. There is no evidence to suggest that using the corner station anemometer instead of the End-X ground anemometer yields more accurate results.

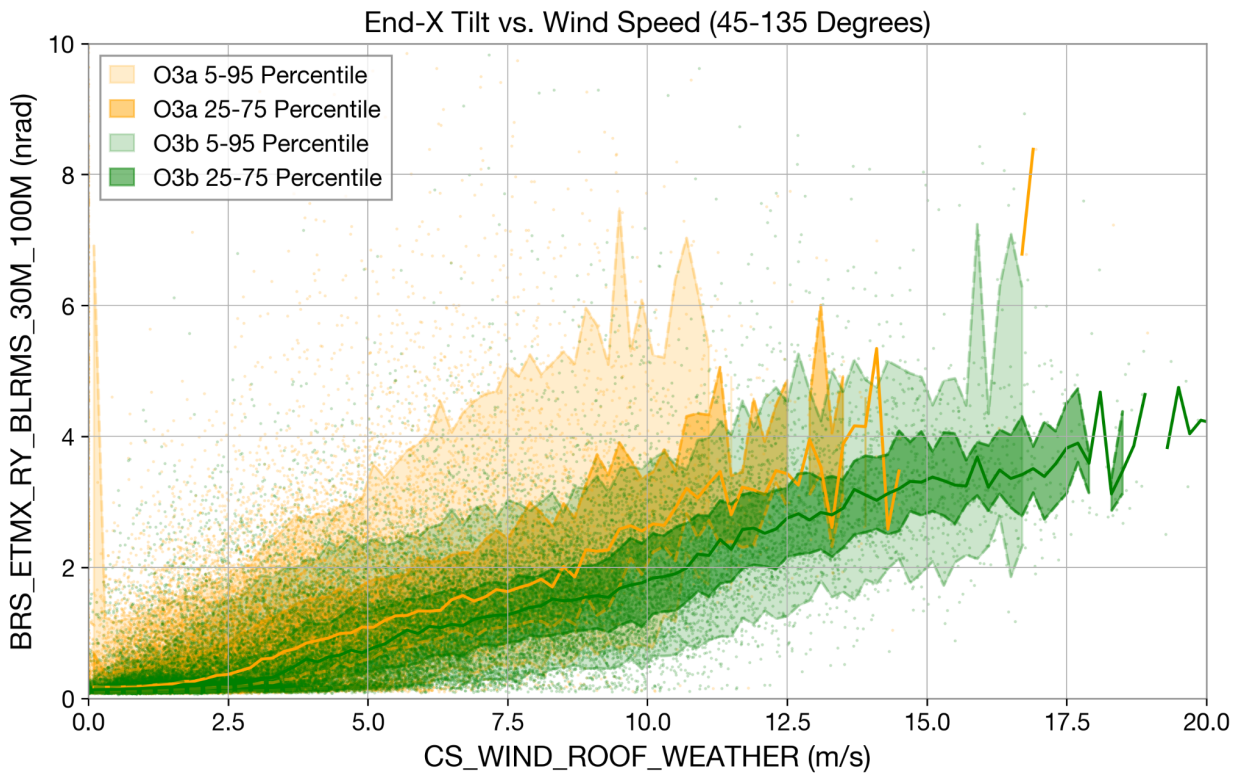

Figure 3.9: Tilt at End-X vs wind speed measured at Corner Station for wind blowing from the -Y direction: Orange and green areas show middle 90 and 50 percent of data from O3a and O3b respectively

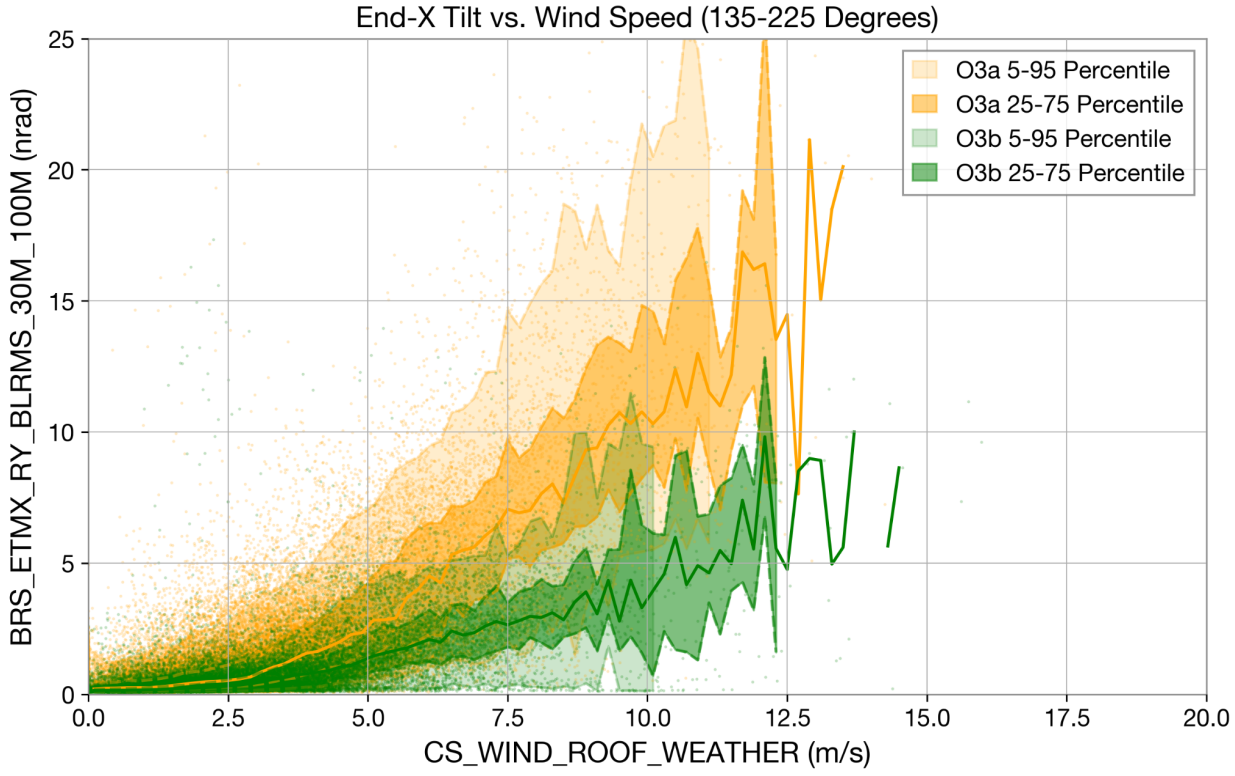

Figure 3.10: Tilt at End-X vs wind speed measured at Corner Station for wind blowing from the -X direction: Orange and green areas show middle 90 and 50 percent of data from O3a and O3b respectively

3.2 Wind Speed vs Tilt at End-Y

We expect much of the results from End-X to apply to End-Y as well. Since the direction sensor at End-Y is known to have reliability issues (it often gets stuck at 0 or with another constant output during lower speed wind conditions) we were unable to use that channel for analysis. Instead we take direction measurements from the corner station anemometer since direction measurements at the corner station are expected to have a strong 1-to-1 correlation with directions measured at the end station.

3.2.1 Tilt at End-Y vs Wind Speed at top of End-Y

Unlike at End-X, comparing the tilt to wind speed at End-Y for all directions (Fig. 3.11) shows we see a significant decrease in between tilt as a function of the rooftop wind speed between O3a and O3b. This indicates either a different relationship between the free stream wind speed and the End-Y roof sensor with fence protection than there is at End-X (ie if the End-Y fence doesn't slow down the wind reaching the anemometer) or a different relationship between the roof-top wind speed and building tilt.

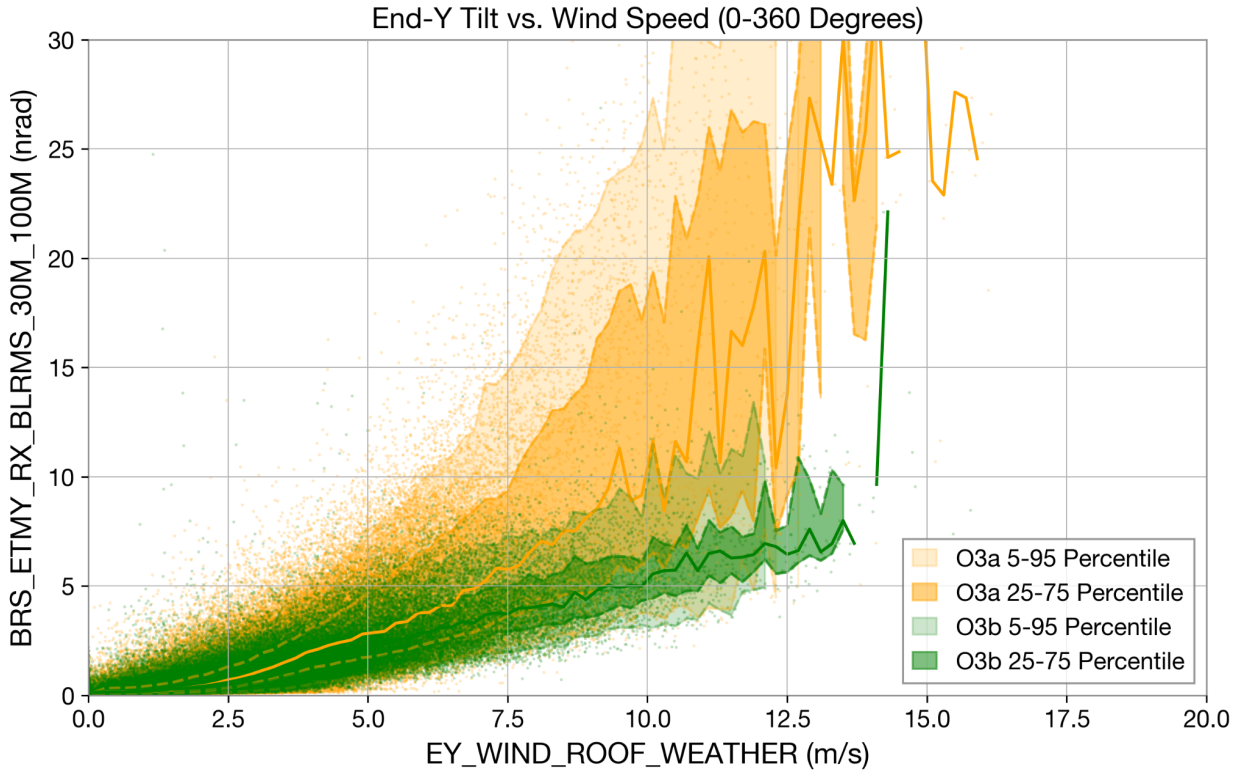

Figure 3.11: Tilt at End-Y vs wind speed measured on top of End-Y: Orange and green areas show middle 90 and 50 percent of data from O3a and O3b respectively

The disaggregated data slows a slight improvement in performance for wind coming from the -Y and a significant improvement for wind coming from the -X (Fig 3.12 and 3.13). This is indicative of either a different relationship between the free stream wind speed and the End-Y roof sensor with fence protection than there is at End-X or a different relationship between the roof-top wind speed and building tilt at End-Y. It is also possible that due to the increased curvature of the End-Y fence towards the north side of the building, the fence provides additional protection against wind coming from the +X direction.

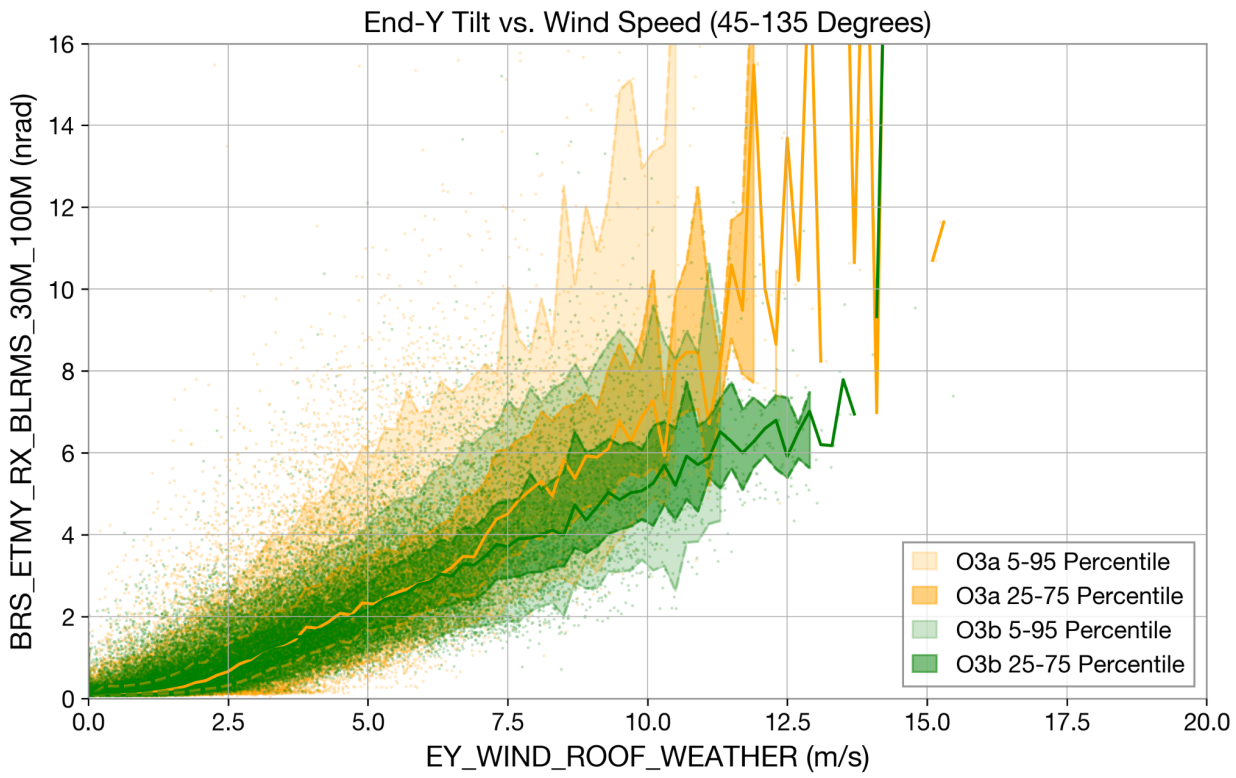

Figure 3.12: Tilt at End-Y vs wind speed measured on top of End-Y for wind blowing from the -Y direction: Orange and green areas show middle 90 and 50 percent of data from O3a and O3b respectively

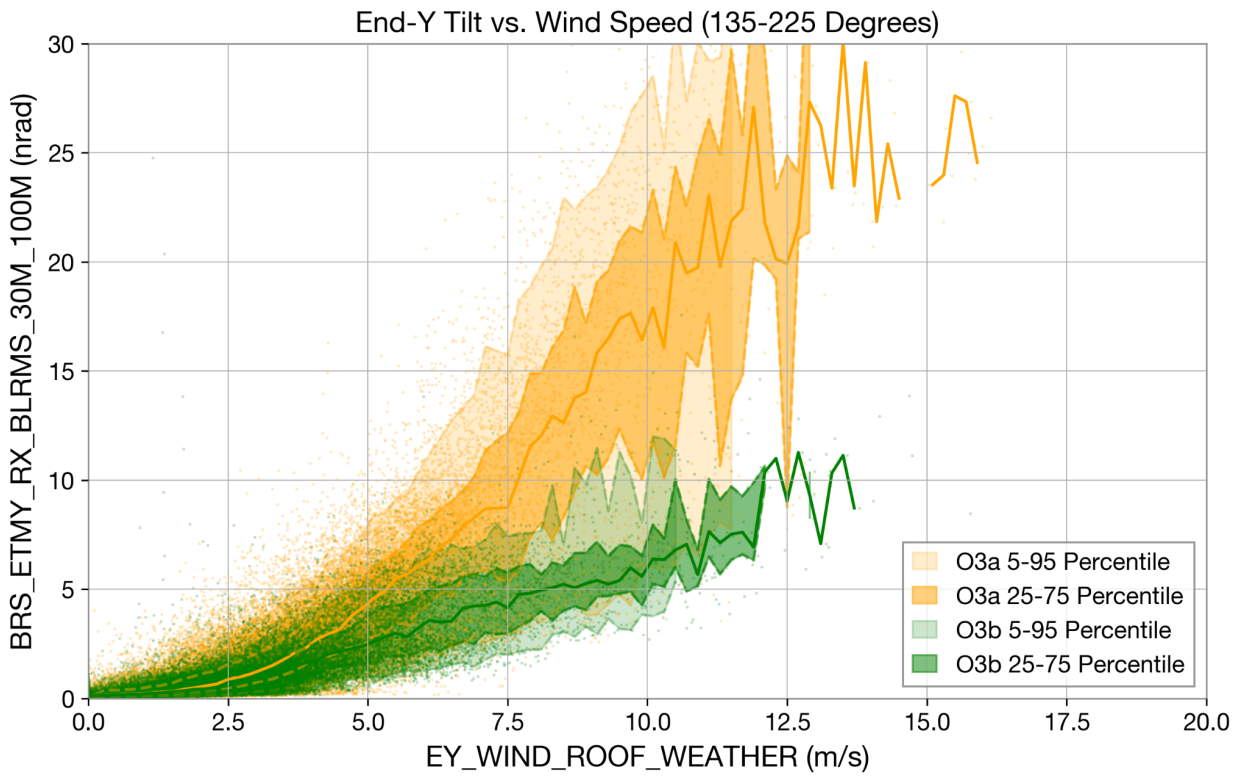

Figure 3.13: Tilt at End-Y vs wind speed measured on top of End-Y for wind blowing from the -X direction: Orange and green areas show middle 90 and 50 percent of data from O3a and O3b respectively

3.2.2 Tilt at End-Y vs Wind Speed at top of Corner Station

Despite the drawbacks that come with using a sensor located 4km away from the location we want the true wind speed for, since the corner station sensor is unaffected by the fence it likely serves as a better point of comparison than the End-Y rooftop sensor.

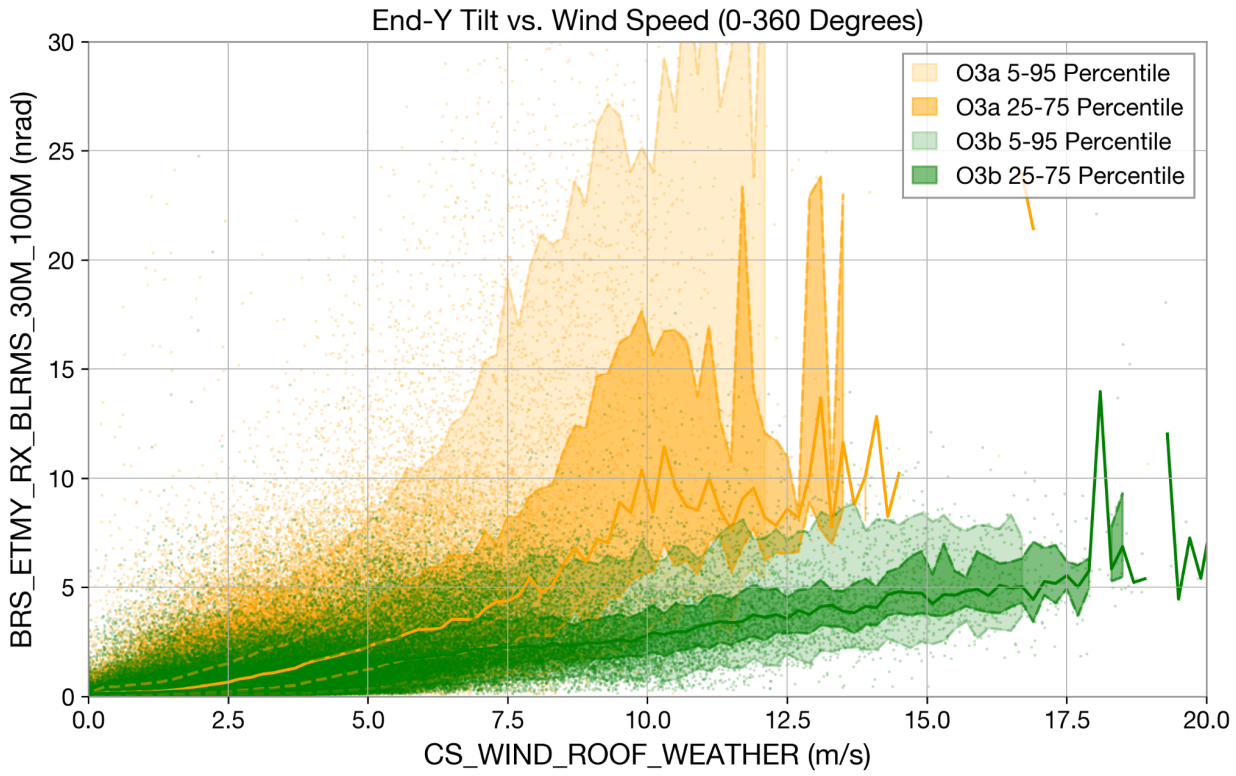

Figure 3.14: Tilt at End Y vs wind speed measured at Corner Station: Orange and green areas show middle 90 and 50 percent of data from O3a and O3b respectively

Looking at wind from the two most significant directions we see that the fence is effective for the expected 45º-135º range (Fig. 3.15). Slightly unexpectedly however, the fence also appears to be effective for wind directions up to about 180º, this result can be seen in Figure 3.16. This is likely due to the increased curvature towards the northern part of the End-Y fence. We suspect that some wind coming from the +X direction is either pushed around the north-east of the observation sensor as wind is redirected around the fence, or that some wind is pulled around the south-west of the observation sensor as a result of a low pressure zone in the region downstream of the wind fence.

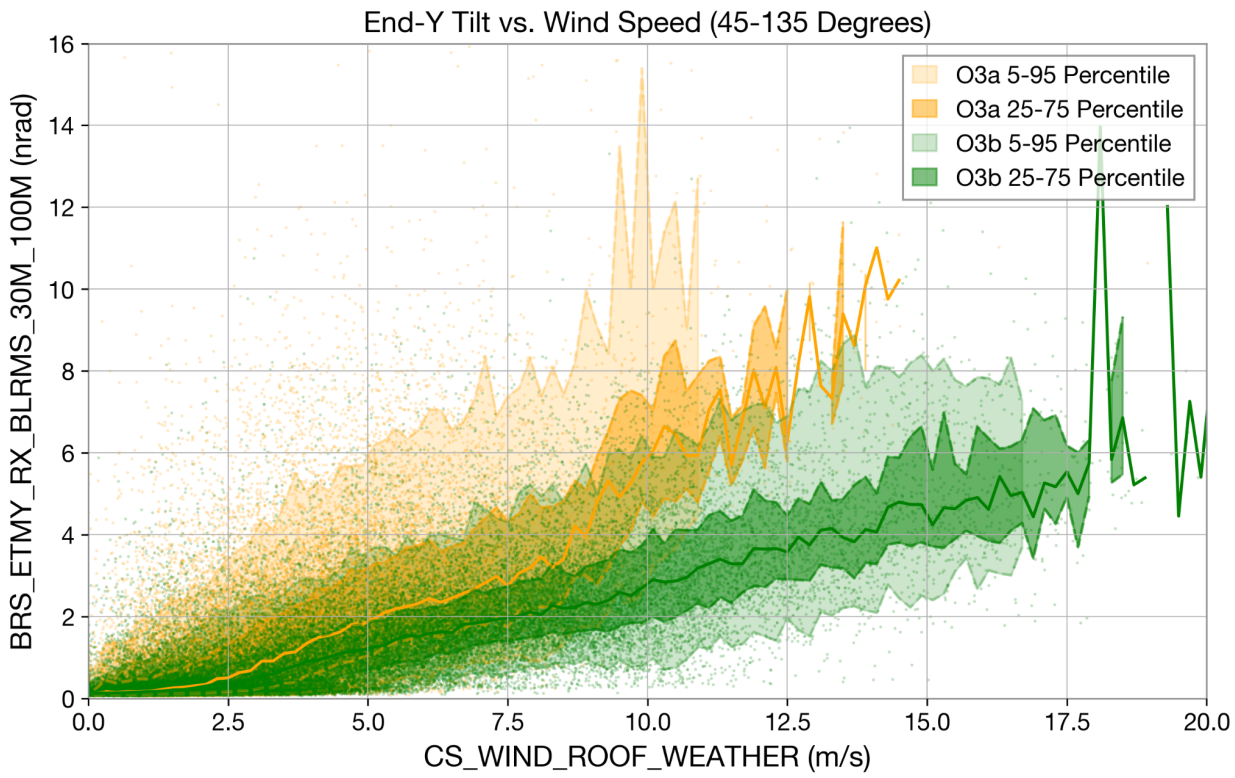

Figure 3.15: Tilt at End Y vs wind speed measured at Corner Station for wind blowing from the -Y direction: Orange and green areas show middle 90 and 50 percent of data from O3a and O3b respectively

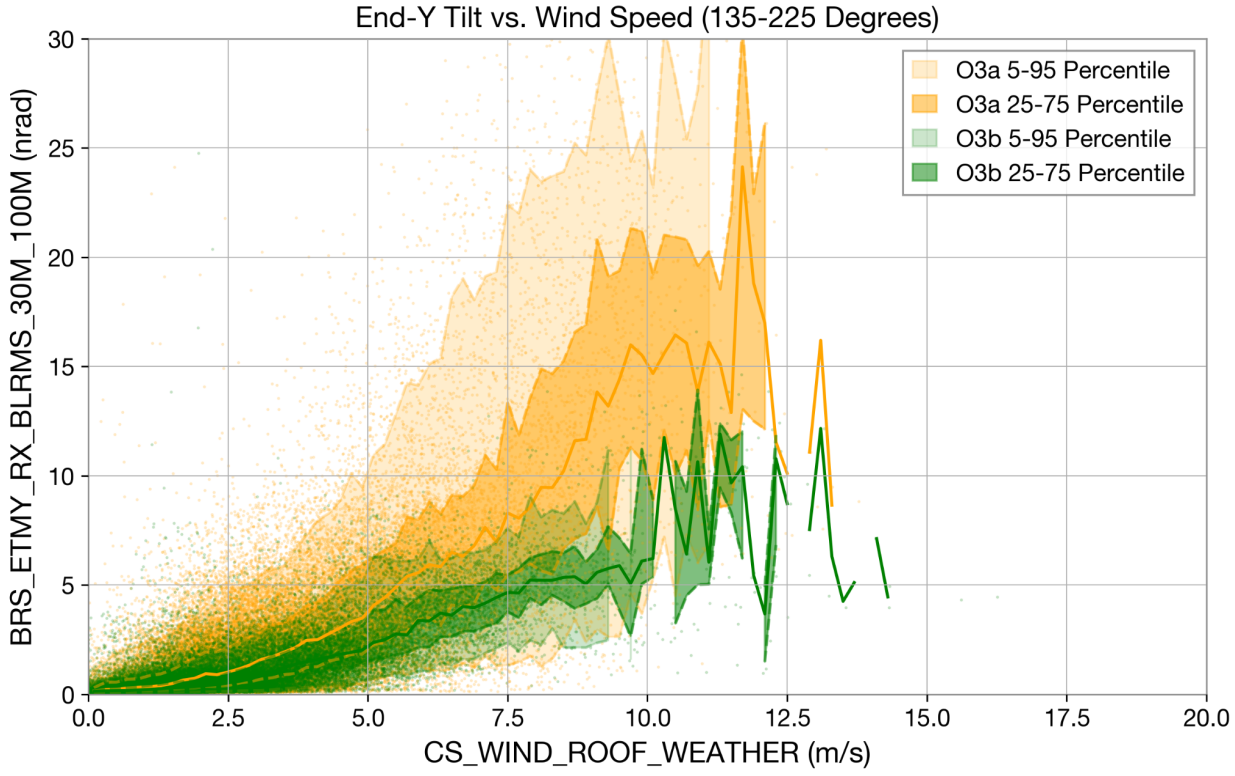

Figure 3.16: Tilt at End Y vs wind speed measured at Corner Station: Orange and green areas show middle 90 and 50 percent of data from O3a and O3b respectively

4. Effect of Wind Fence on Perceived Ground Motion

Having established the efficacy of the fence in reducing the tilt for wind coming from the protected direction, this section will look directly at horizontal motion measured during times of low seismic activity (30-100mHz ITMY-Z motion <80 nm/s) as a function of wind to determine the control system benefits derived from the wind fence.

4.1 End Station STS-2 Motion vs. Wind Speed

Since motion measured by the STS-2 sensors has two predominant sources: tilt, and true ground motion (ie the microseism and earthquakes), for this study we want to isolate the effects of tilt. To do so we focus on all data points for which the 30-100 mHz BLRMS motion as measured by the ITMY sensor in the Z direction is < 80 nm/s. Since tilt coupling affects only the X and Y directions while earthquakes typically excite all axis of motion, time periods which feature low motion in the Z direction are likely to correlate to motion which is primarily driven by tilt-coupling effects or is limited to ambient ground motion. Thus plotting this subset of end station STS-2 motion as a function of wind speed yields very similar results as plotting tilt as a function of wind speed. Due to the very strong correlation between this data and the data shown in *Section 3*. This section will only contain some notable highlights.

Plotting End-X STS-2 motion against wind speed (Fig. 4.1) we see relatively little improvement in STS-2 performance between O3a and O3b, with the only significant improvement coming from high speed winds >~8 m/s. However it is worth noting that the STS-2 motion observed at End-X during high wind speed periods remains significantly lower than that at End-Y, even after the installation of the fence.

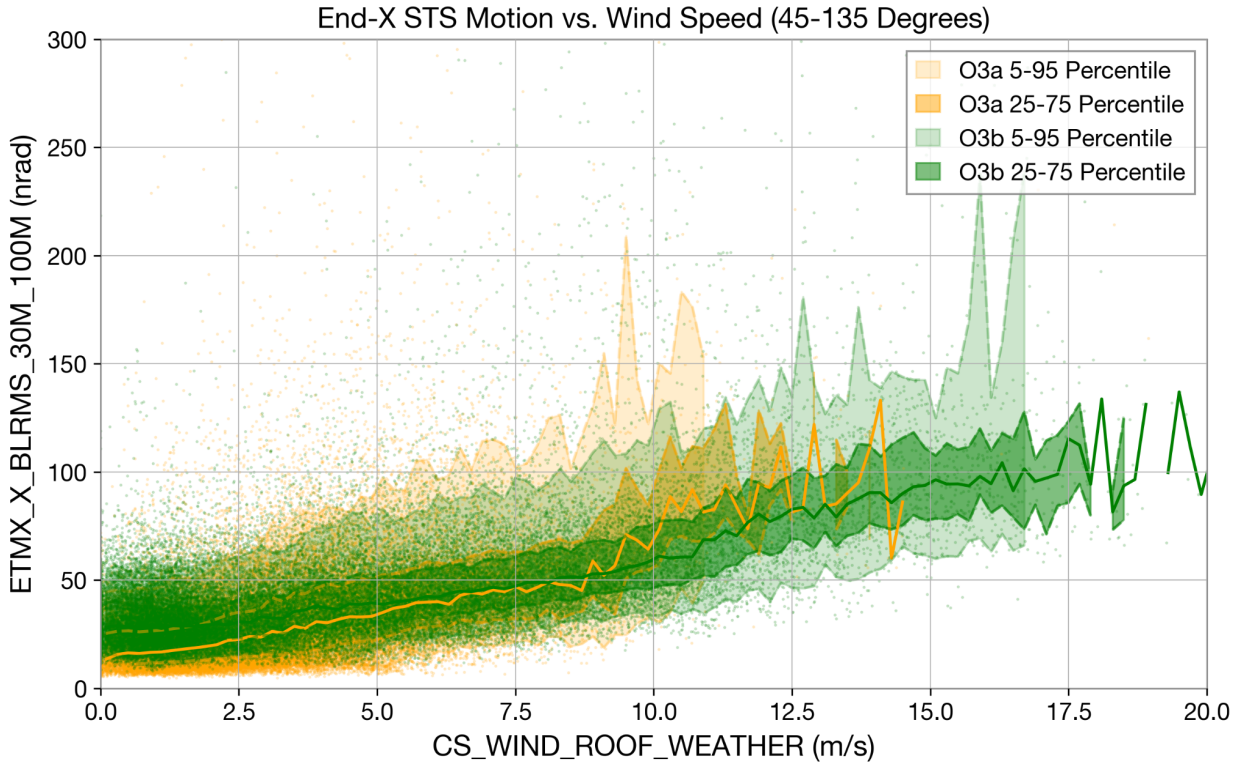

Figure 4.1: STS Motion at End X vs wind speed measured at Corner Station for wind blowing from the -Y direction: Orange and green areas show middle 90 and 50 percent of data from O3a and O3b respectively

In contrast to Figure 4.1, Figure 4.2 shows a very significant improvement in End-Y STS-2 performance as a function of wind speed between O3a and O3b. In this case we see noticeable improvements for winds >~2m/s with almost a 2 factor improvement at higher wind speeds >~8m/s.

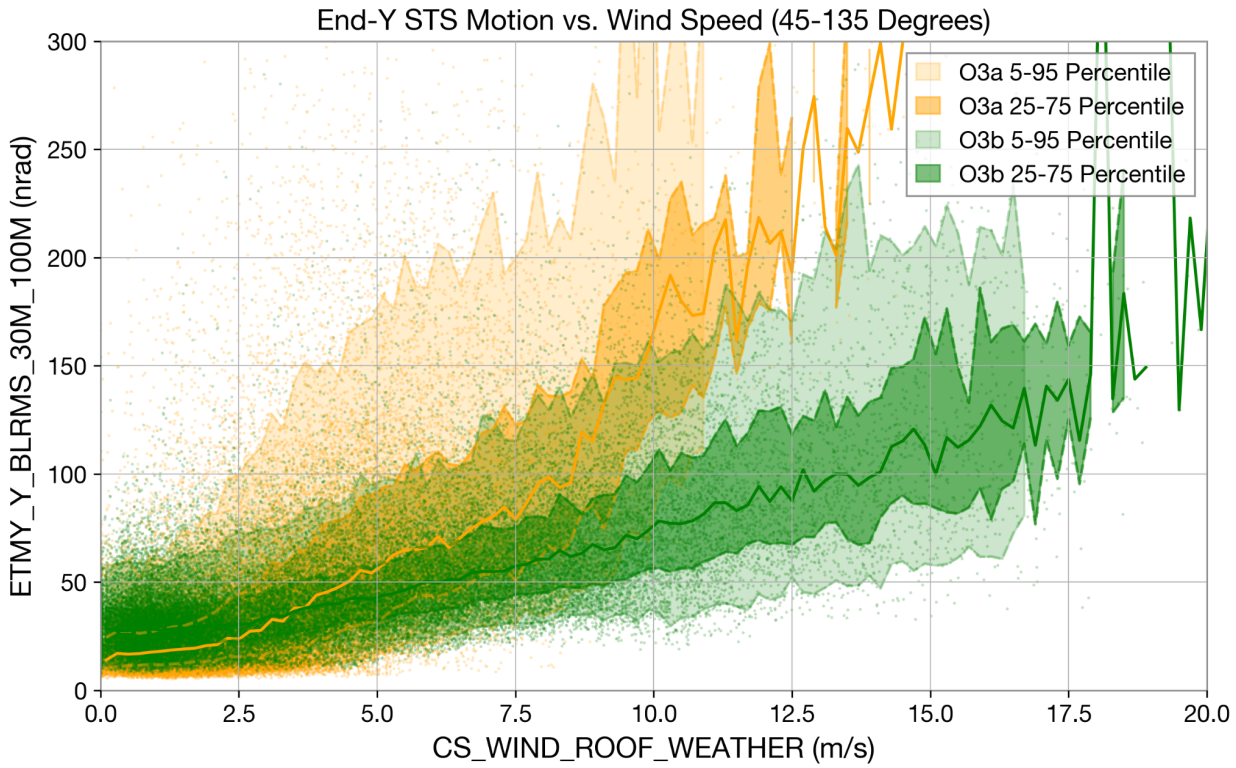

Figure 4.2: STS Motion at End Y vs wind speed measured at Corner Station for wind blowing from the -Y direction: Orange and green areas show middle 90 and 50 percent of data from O3a and O3b respectively

4.2 End Station Tilt-Subtracted STS-2 Motion vs Wind Speed

We will now plot the tilt-subtracted STS-2 motion as a function of corner station wind speed. The goal of this section is to attempt to determine when wind begins to have an impact on the control system and whether this changed as a result of the wind fence or not.

Figure 4.3 shows the End-X tilt subtracted motion as a function of corner station wind speed. In this plot we can see that O3b saw an increase in ground motion during low-wind periods. This is likely a result of the microseism which tends to be more active in the winter (ie O3b) and can be observed in the 30-100mHz bands. However looking at the slope of the two lines we see that wind has a much smaller impact during O3b than during O3a. During O3a almost any wind regardless of how fast had some effect on the tilt-subtracted motion, and wind speeds >~8 m/s had a significant impact on motion. However, during O3b wind only starts having a noticeable effect on motion around 2.5 m/s and this effect remains relatively minimal even for higher wind speeds.

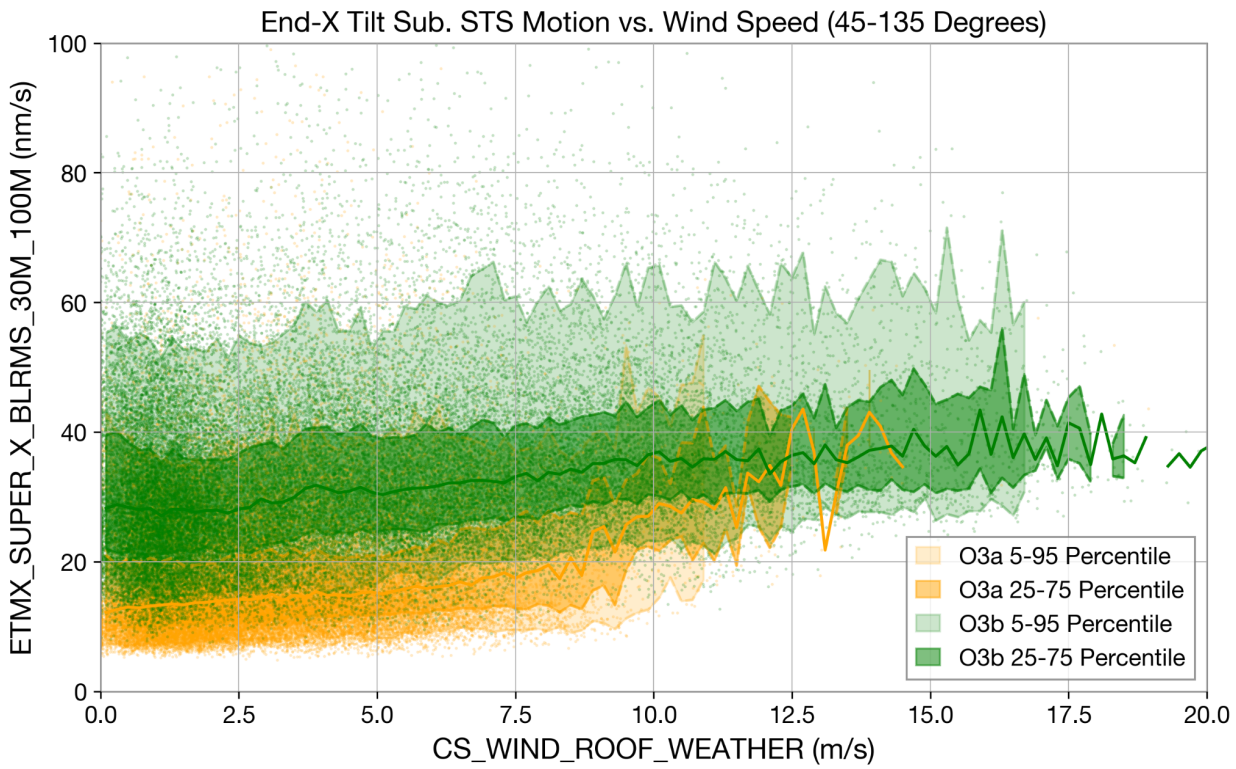

Figure 4.3: Tilt-subtracted STS Motion at End X vs wind speed measured at Corner Station for wind blowing from the -Y direction: Orange and green areas show middle 90 and 50 percent of data from O3a and O3b respectively

Figure 4.4 shows the End-Y tilt subtracted motion as a function of corner station wind speed. We once again see the increase in ambient motion during O3b. However once again we see that wind has a much smaller impact during O3b than during O3a. During O3a almost any wind regardless of how fast had some effect on the tilt-subtracted motion, and wind speeds >~8 m/s had a significant impact on motion. However, during O3b wind only starts having a noticeable effect on motion around 2.5 m/s and this effect remains relatively minimal even for higher wind speeds.

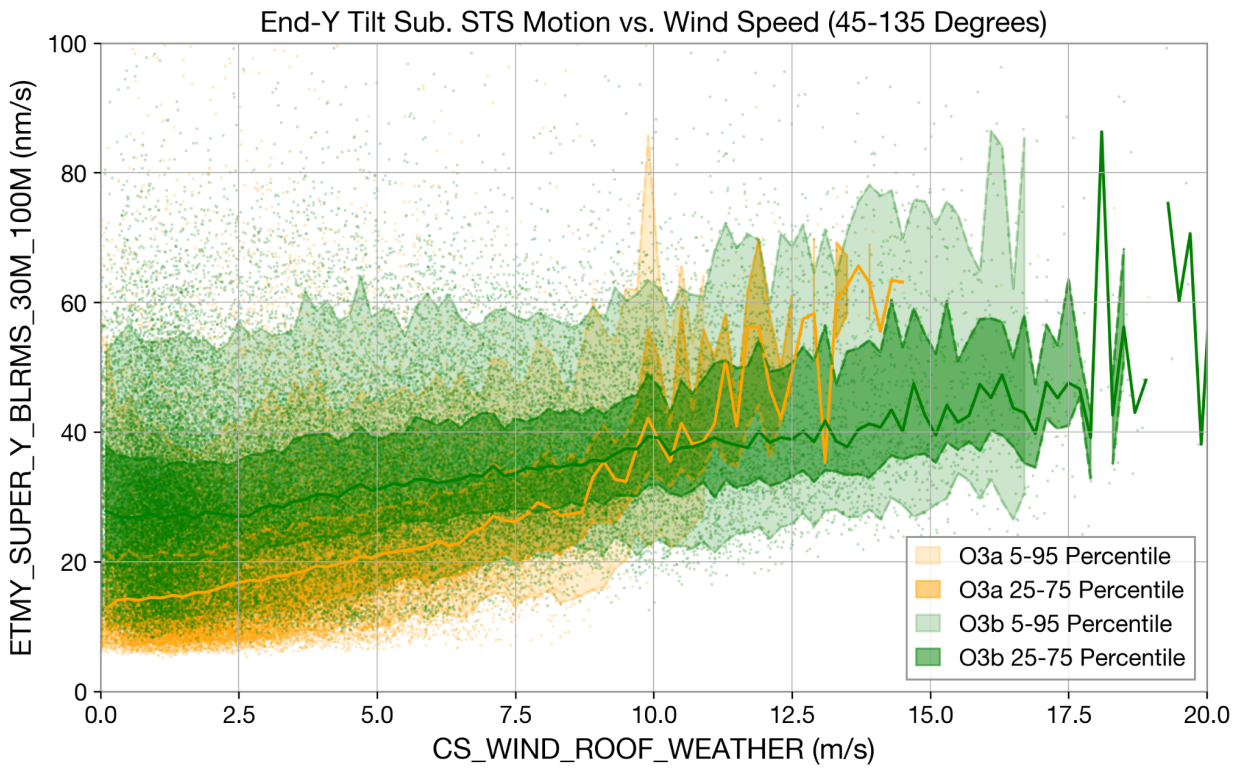

Figure 4.4: Tilt subtracted STS Motion at End Y vs wind speed measured at Corner Station for wind blowing from the -Y direction: Orange and green areas show middle 90 and 50 percent of data from O3a and O3b respectively

The overall increase in ground motion between O3a and O3b could be due to environmental factors, such as a larger microseism due to larger off coast storms during the winter season, rather than local factors which we would expect to be mitigated by the BRS tilt-subtraction.

5. Reduction of Tilt Standard Deviation Due to Wind Fence

It has been speculated that short spikes in observation station motion are more detrimental to interferometer performance than periods of sustained but moderate motion.Thus it could be useful to evaluate what effect, if any, the wind fence has on the distribution of tilts during similar wind periods.

This section attempts to evaluate this question by considering the normalized standard deviation of rotation data for each .25 m/s range of wind speeds. In order to account for differences in sample size between O3a and O3b as well as to better evaluate the statistical significance of our results, we use a bootstrap sampling approach. For each .5 m/s of wind speed we take 500 bootstrap samples of size equal to 80% of the smaller original sample (for example if we had 500 minutes of wind speeds between 6.0 and 6.5 m/s during O3a and 1000 minutes during O3b, each bootstrap sample would have 400 data points). We ultimately find some evidence to indicate that normalized standard deviations in tilt were reduced as a result of the wind fence but cannot make any concrete conclusions with the available data.

It is possible that reduction in the standard deviation of tilt values is a result of the fence stabilizing the flow of wind passing through it. Previous modeling work supports this conclusion [HOF18]. We also have qualitative evidence to support this effect of the fence in the form of a smoke test in which smoke from a

candle upstream of the fence appeared to flow in a less turbulent manner after passing through the fence [ALOG39564]. However due to limitations in instrumentation we have yet to be able to verify this quantitatively.

5.1 Reduction of Variance at End-X

In this section we look at time periods during which wind was blowing from the +Y direction since this is the direction from which the wind fence has a significant impact. The following figures show various measures of standard deviation. Each point of the following graphs represents data from a .25 m/s bin of wind speed. For example a green point at (3.875 m/s, .5 nrad) in Figure 5.4 means that the magnitude of building tilt during all time periods when the wind speed was between 3.75–4.0 m/s during O3b had a standard deviation of .5 nrad. For Figure 5.2 and 5.3 the same binning method is used, but instead of plotting the middle speed of each bin on the X axis, we plot the mean building tilt of each bin. A visualization of this binning method is shown in Figure 5.1.

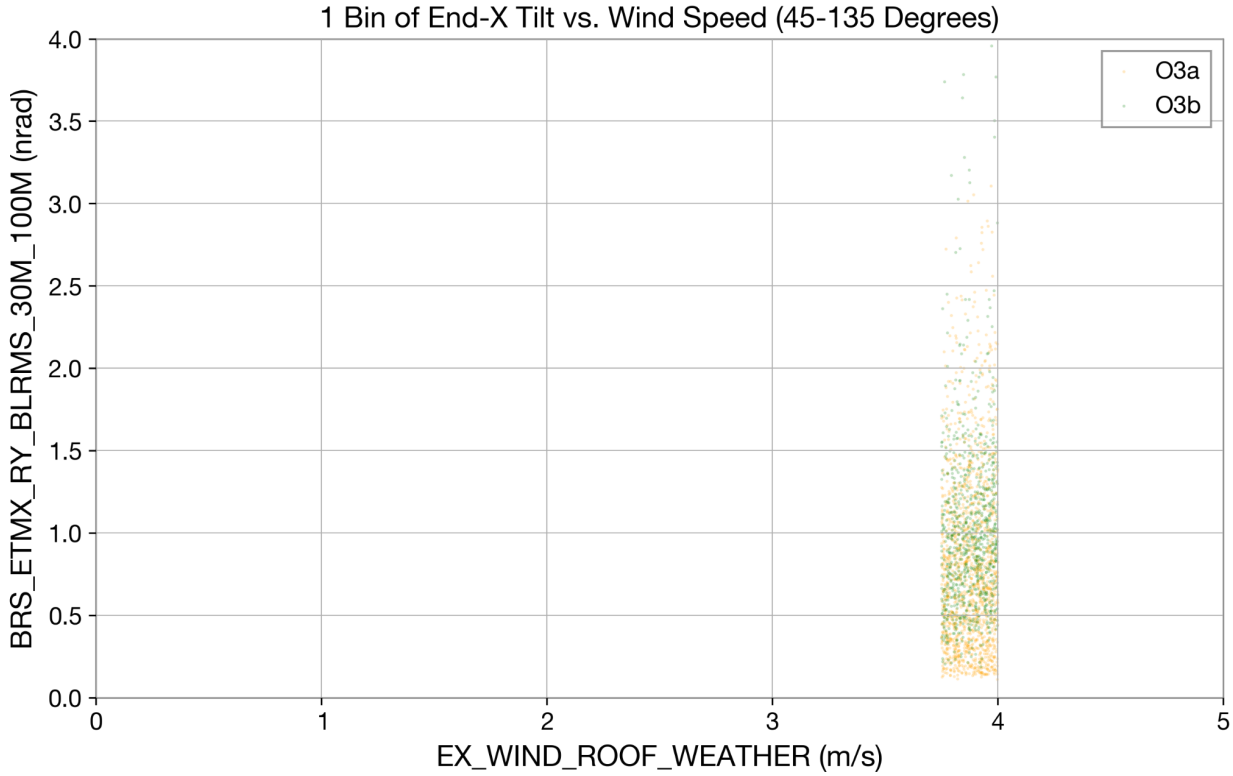

Figure 5.1: 1 bin from the End-X Tilt vs wind speed plot. Values of average wind speed, average tilt, and bootstrapped standard deviation from this bin correspond to a single data point on the remainder of the figures in tbis section

Looking at Figure 5.2, a few trends are particularly notable. In O3b the standard deviation of tilts stays constant for wind > ~5m/s whereas during O3a standard deviations of tilts consistently increased as wind speed did. However, normalizing the standard deviation values with respect to the sample means show very little reduction in normalized standard deviation, if any (Fig. 5.3). This indicates that most of the perceived reduction in standard deviation is actually a consequence of tilt in general being reduced during O3b.

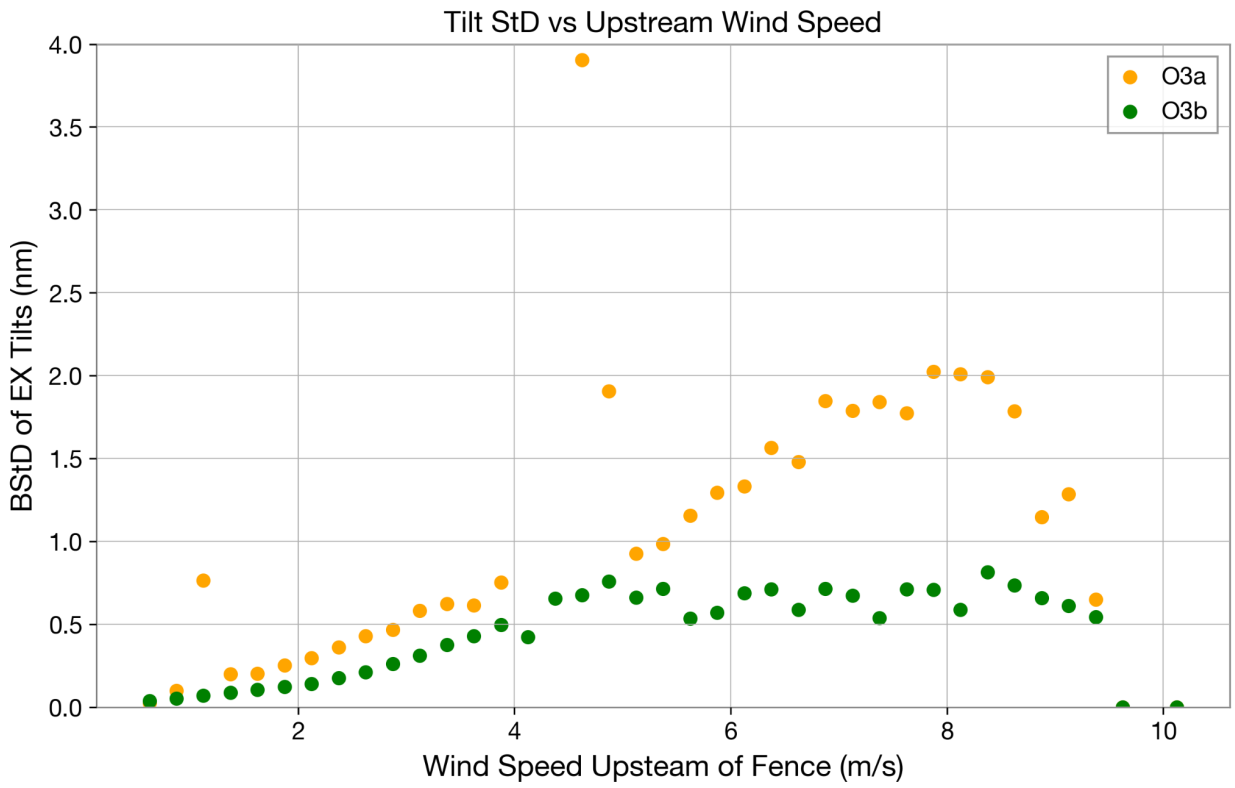

Figure 5.2: Bootstrapped standard deviation of End-X tilts vs average wind speed for each wind speed bin

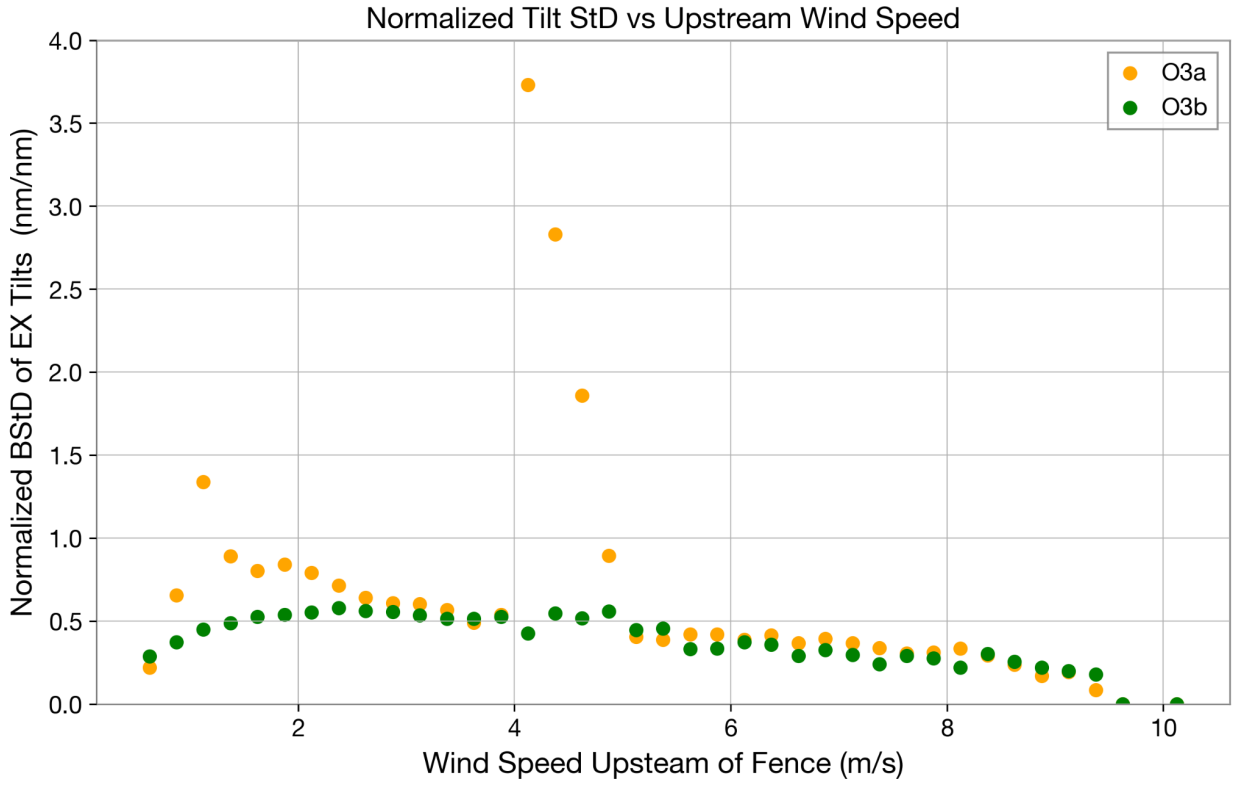

Figure 5.3: Normalized bootstrapped standard deviation of End-X tilts vs average wind speed for each wind speed bin

We see a similar trend when plotting tilt standard deviation against the average tilt (Fig. 5.4). The standard deviation of tilts reaches a maximum and stays constant for average tilts > ~1.2 nrad during O3a, whereas during O3a tilt standard deviations continued increasing as tilt increased. However, once again plotting the normalized standard deviation (Fig 5.5) indicated that the reduction in standard deviation might be less significant than it appears in Figure 5.4.

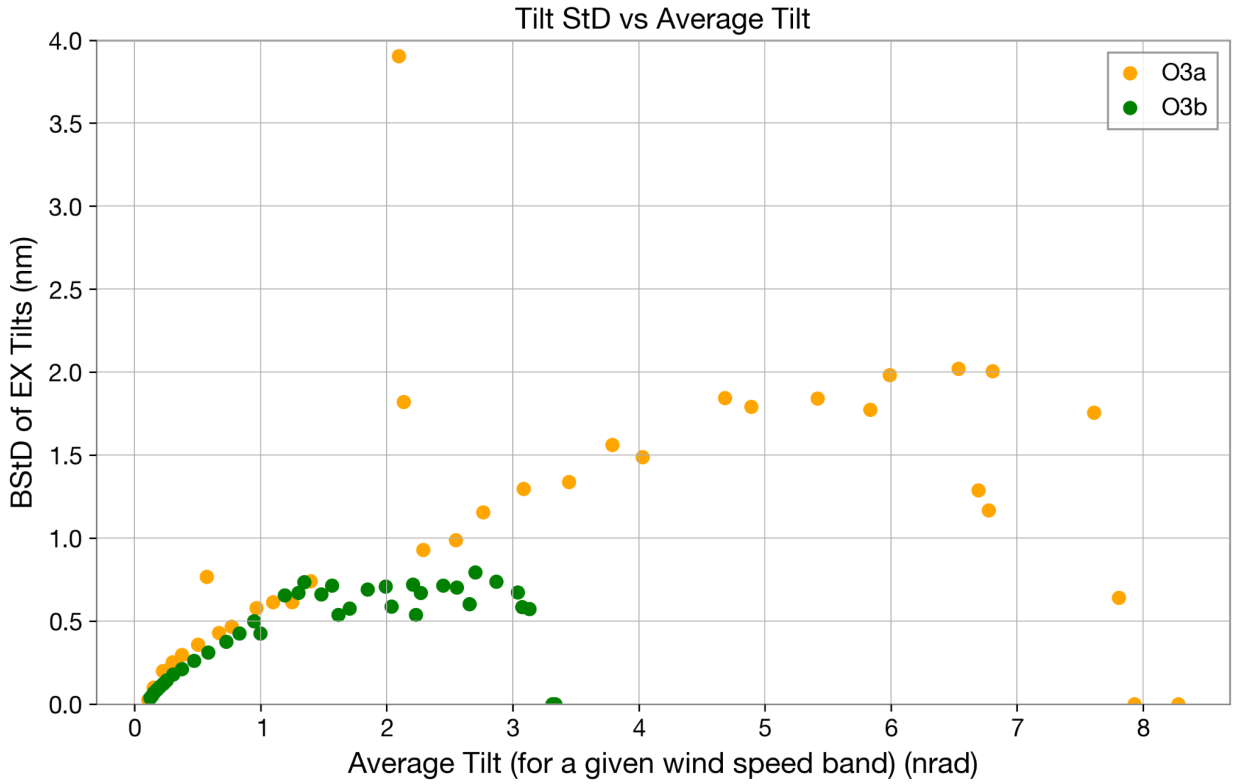

Figure 5.4: Bootstrapped standard deviation of End-X tilts vs average tilt for each wind speed bin

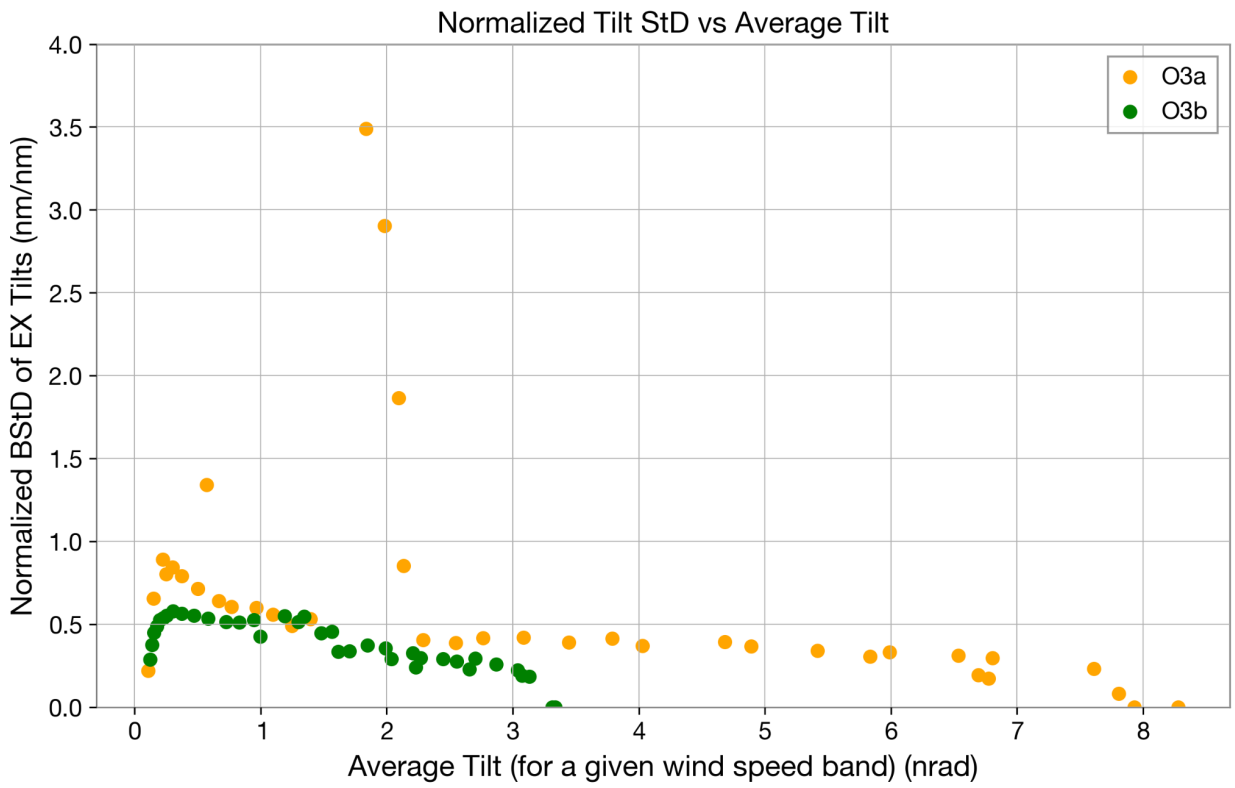

Figure 5.5: Normalized ootstrapped standard deviation of End-X tilts vs average tilt for each wind speed bin

One additional feature that is noticeable in Figure 5.3 and Figure 5.5 is that during both O3a and O3b, the normalized standard deviation increases as wind speed/tilt does for relatively small amounts of wind/tilt until reaching a peak around 2 m/s wind speed corresponding to around 1.4 nrad tilt. We suspect that this point marks the point where wind becomes the primary contributing factor to the magnitude of tilt over ambient ground motion. To properly evaluate this claim it would be useful to have additional anemometers to measure free stream wind as well as additional seismometers outside the building to measure ambient ground motion such as that in [LHO Log 19210].

5.2 Reduction of Variance at End-Y

The following plots follow the same format and the same procedure for generating the previous 4 plots. However for these plots we look at tilts and End-Y as well as the wind speed/direction as measured at the corner station.

Looking at End-Y tilt standard deviation as a function of wind speed, we see a reduction in the standard deviation across the full range of wind speeds, however once again this difference is reduced to near negligible amounts once normalizing the standard deviations of tilt by the mean tilt.

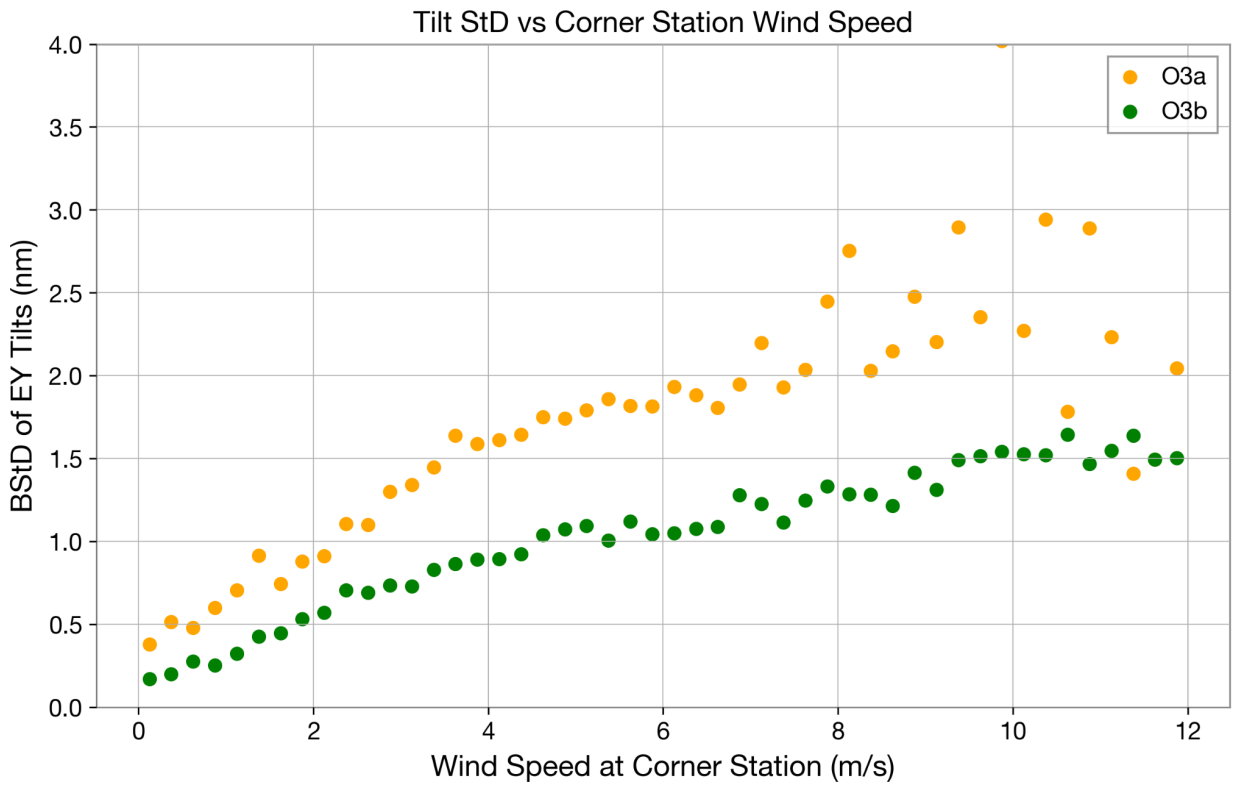

Figure 5.6: Bootstrapped standard deviation of End-X tilts vs average wind speed for each wind speed bin

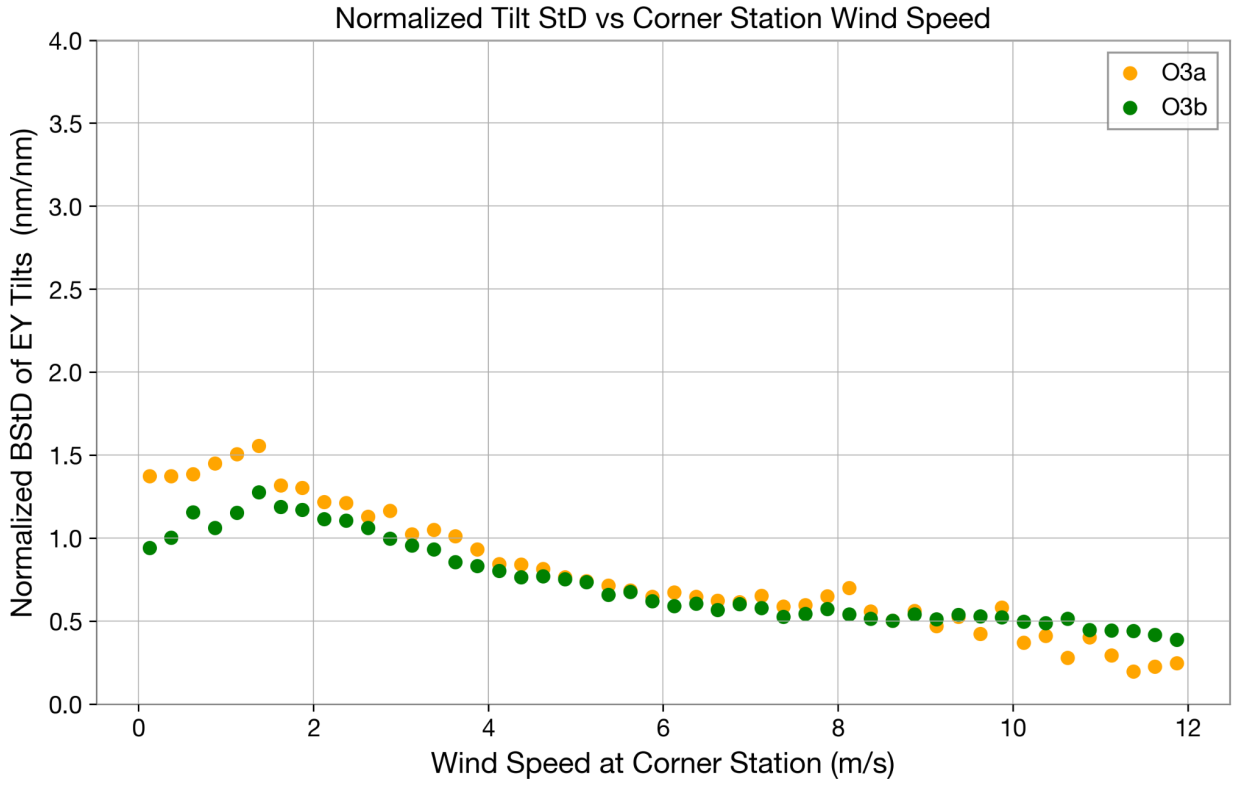

Figure 5.6: Normalized bootstrapped standard deviation of End-X tilts vs average wind speed for each wind speed bin

Looking at standard deviations as a function of mean tilt, plotting (normalized) standard deviation against the average tilt for each wind speed bin does actually show a significant decrease in the standard deviation of tilt during O3b (Fig. 5.7) even when normalizing for the average tilt (Fig. 5.8). However, some unreliability is introduced in these results since we were forced to use the corner station anemometer due to the lack of an anemometer at End-Y which is reliable and not affected by the fence.

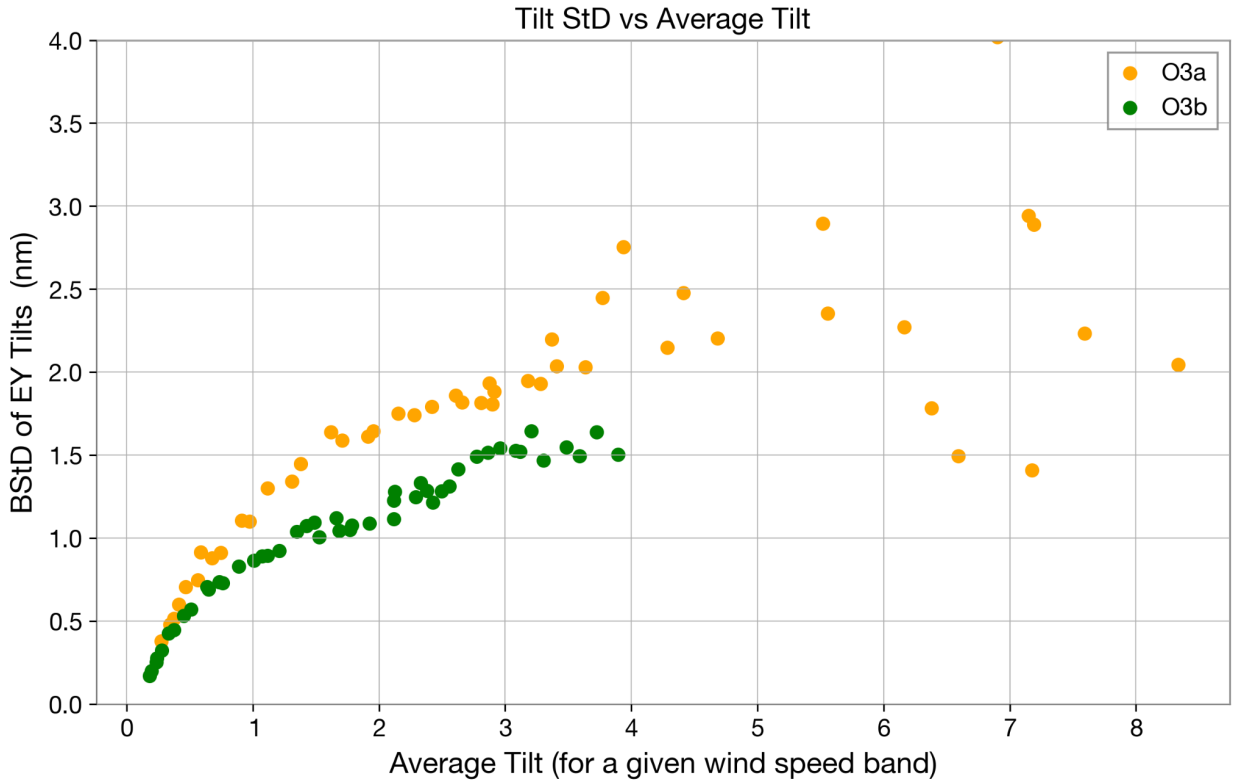

Figure 5.7: Bootstrapped standard deviation of End-X tilts vs average tilt for each wind speed bin

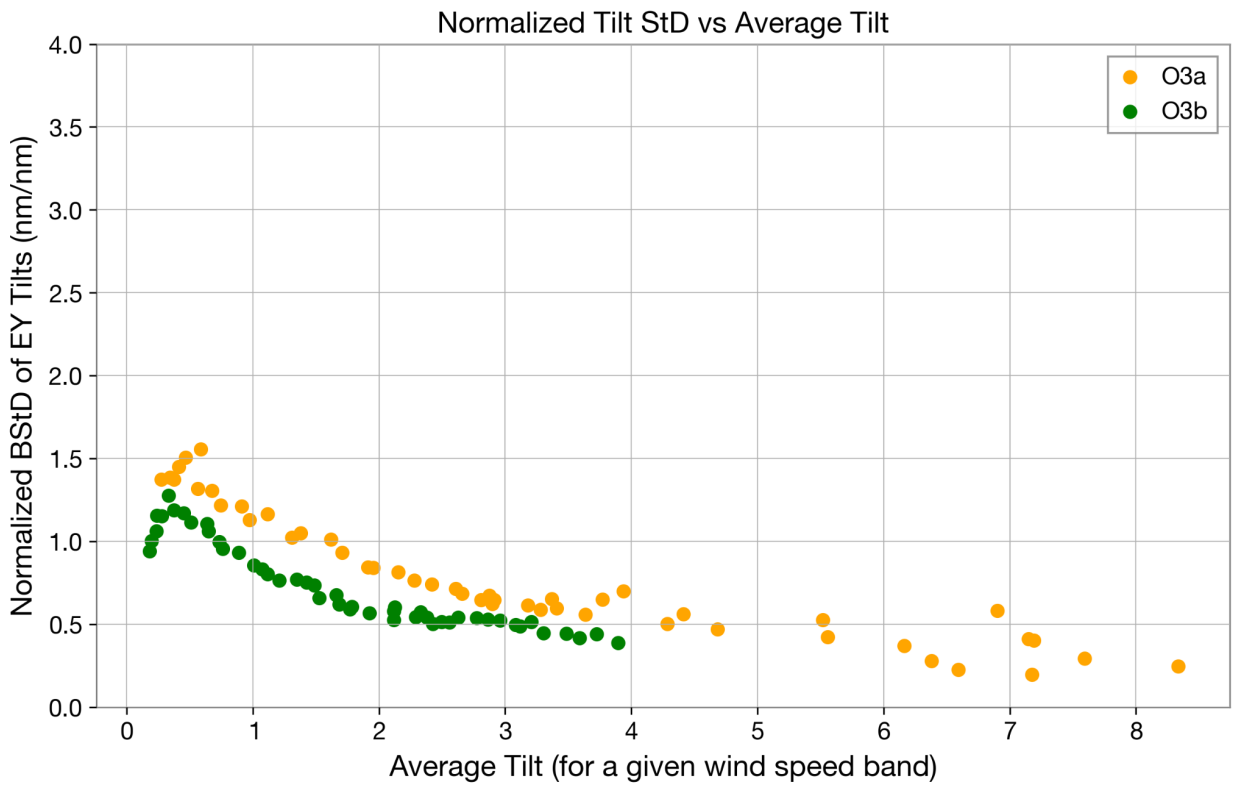

Figure 5.8: Normalized bootstrapped standard deviation of End-X tilts vs average tilt for each wind speed bin

We also notice a similar trend as we did at End-X with normalized tilt standard deviations increasing to a maximum then proceeding to decrease, which suggests that this indeed a global trend resulting from global factors such as ground motion and wind rather than a trend localized to just End-X. In this case we see the maximum normalized standard deviation is reached at wind speeds of around 1.5 m/s and tilts around .4 nrad. Once again we expect that this is the point at which wind becomes the dominant factor contributing to tilt but we lack the instrumentation to properly test this claim.

6. Relative Impact of Wind on Ground Motion at all Observation Stations

Having confirmed the efficacy of the wind fences it is now useful to compare the effects of wind on each relevant observation station/sensor to identify potential future points of improvement. First, we look at the distribution of 30-100MHZ BLRMS ground motion during high wind (>6 m/s) times as measured by the ITMY sensor as well as the end station STS-2 sensor, both tilt subtracted and raw channels. The results are shown in Figure 6.1.

Despite a significant increase in high speed wind in O3b over O3a, in Figure 6.1 we see a clear reduction in the detected ground motion from the End-X STS-2 Sensors (shown in blue). The average motion measured in O3b being about 67 nm/s while the average motion measured in O3a was about 120 nm/s. We also see that motion measured by the non-tilt-subtracted sensors (shown in green) is slightly reduced in 2020 compared to 2019 with an average of about 62 nm/s in 2019 and 59 nm/s in 2020. These histograms also show a significant change in the tail of the distribution for End-X. During O3a, the tail for the non-corrected motion at End-X is much longer than for the corner station, but during O3b, the high-motion tail for the floor motion at End-X is greatly reduced, and becomes much closer to the motion

seen in the corner station. With tilt-correction, we see that the distribution of motion at End-X is clearly below the X motion in the corner station.

Although Figure 6.1 gives us a good overview of the data, it may obscure more subtle changes resulting from the wind fence. Thus it is helpful to treat this plot as motivation for the remainder of the plots in this section rather than try to draw conclusions directly from it.

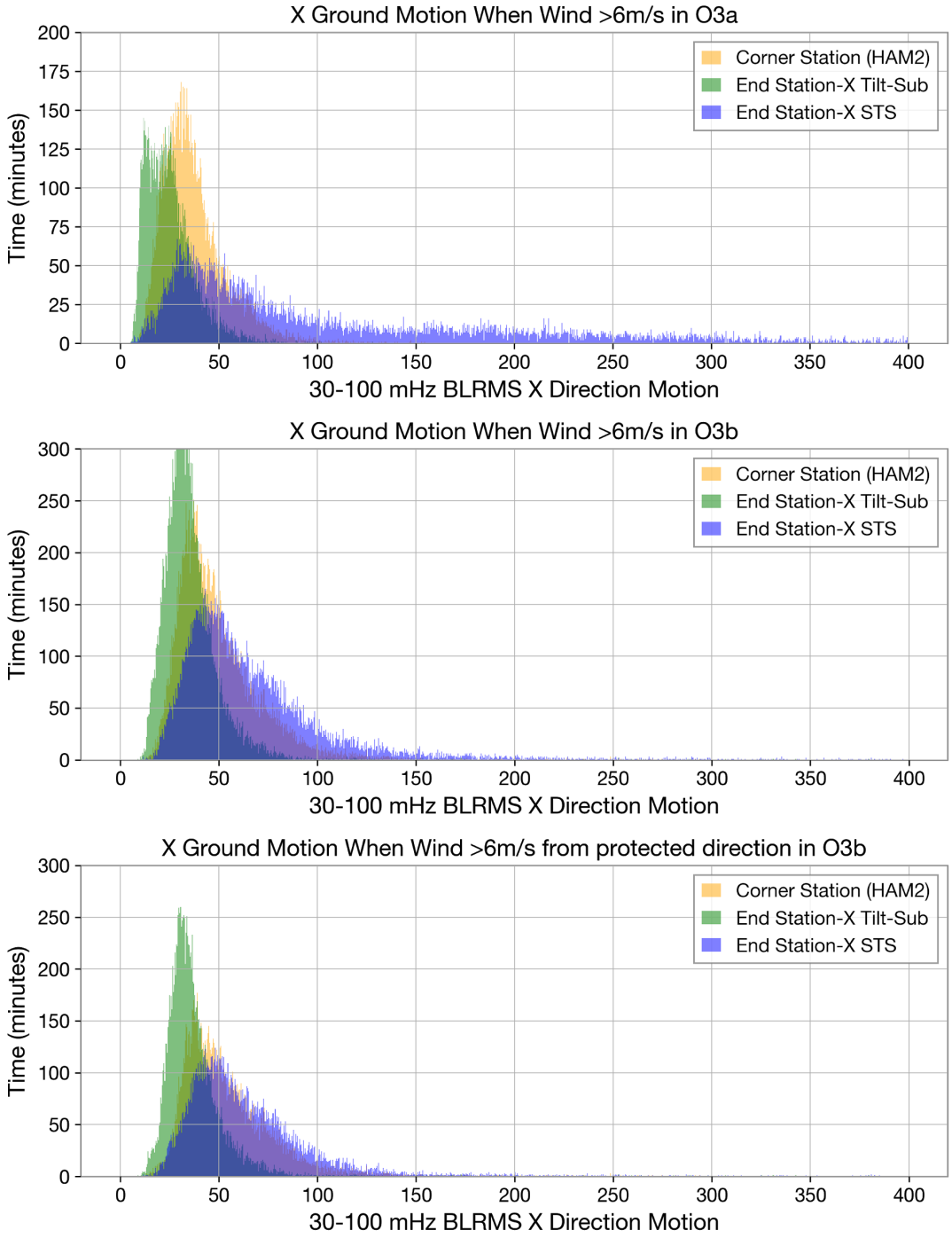

Figure 6.1: 30-100 mHz BLRMS X Direction Motion as Measured by ITMY (yellow), End-X STS (blue), End-X Tilt Subtracted (green)

6.1 End Station STS-2 vs ITMY Motion

It is useful to compare the performance of STS-2 sensors at the end stations with the ITMY sensor as these are identical seismometers which are affected differently by tilt coupling effects due to differing proximities to building walls as well as the different size/shape of the building itself. More specifically, the ITMY sensor is less affected by tilt coupling effects due to an increased distance between the sensor and the corner station building walls compared to the distance between the end station STS-2 sensors (both End-X and End-Y). This section looks at motion measured simultaneously by these sensors during high wind speed periods.

6.1.1 30-100 mHz BLRMS STS-2 Motion at End-X vs. ITMY

Plotting motion at the end stations vs the corner station during O3b gives us an idea of the current effects of wind on Hanford's seismic isolation systems. Figure 6.2 shows a plot of X-direction STS-2 End-X motion against the ITMY X-direction with each data point representing a minute of data when the wind at the corner station was faster than 6 m/s and the Z-direction 30-100mHz motion at the corner station was less than 80 nm/s. The color of each point represents the average wind speed during that time period, the darker colors correspond to the slower wind (min 6 m/s) and the lighter colors correspond to the faster wind (max 24 m/s). Best fit lines for the data are plotted in blue (note that these lines are included to better understand the density of the data distribution rather than representing an accurate model of the data) and the grey lines represent the line y=x.

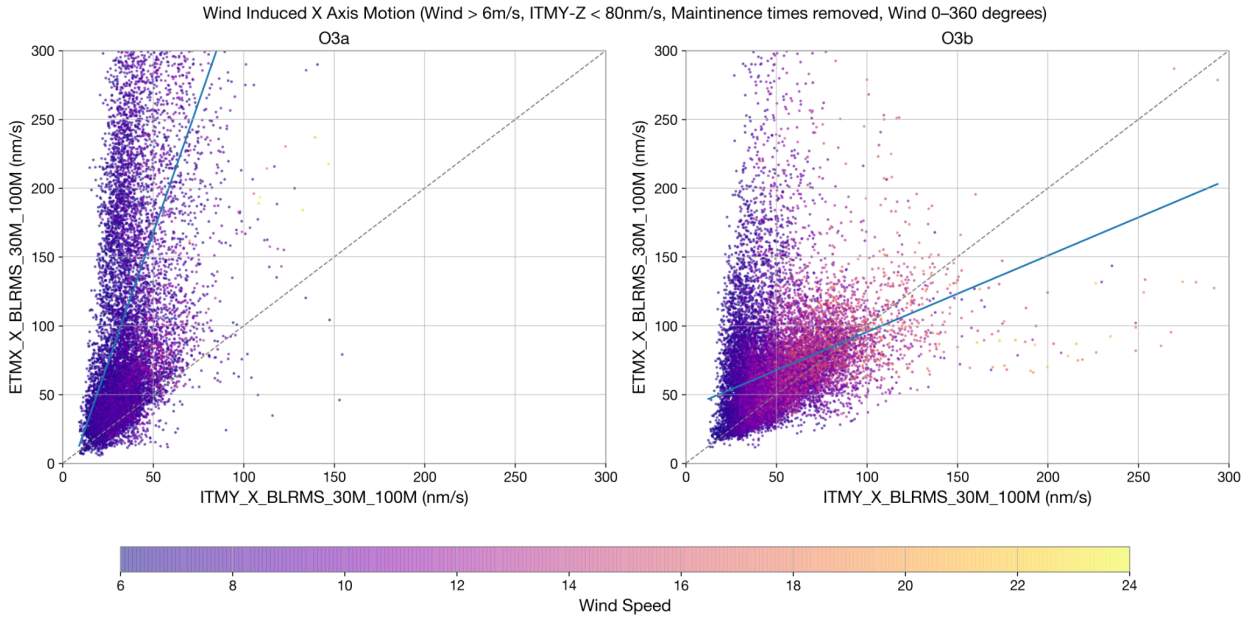

Figure 6.2: Relative performance of ITMY-X and EX STS-2 sensors during O3a and O3b. Lighter colored points indicate faster wind

From this plot it is apparent that there has been a reduction in X-direction motion at the end station relative to the corner station between O3a and O3b. Examining the shape of the distributions as well as the best fit lines we see that whereas during O3a the End-X STS-2 sensor almost always detected (often significantly) more motion than the ITMY sensor. During O3b the End-X STS-2 and ITMY sensors generally observed similar amounts of motion. The best fit line of the O3b subplot suggests that during higher wind times the End-X STS-2 often measured less motion than the ITMY sensor.

Disaggregating these results based on the direction of wind gives even more evidence regarding the efficacy of the wind fence. Figures 6.3 and 6.4 show a similar reduction as we saw in Figure 6.2. Since the wind direction (as measured at the corner station) fell between 45º-135º about 78% of the time we expect the O3b trend from Figures 6.3 and 6.4 to dominate the trend we observe in Figure 6.2**.** Although O3a only saw wind coming from the 45-135 direction about 34% of the time, there is also less of a distinction between this and other directions due to the lack of a wind fence.

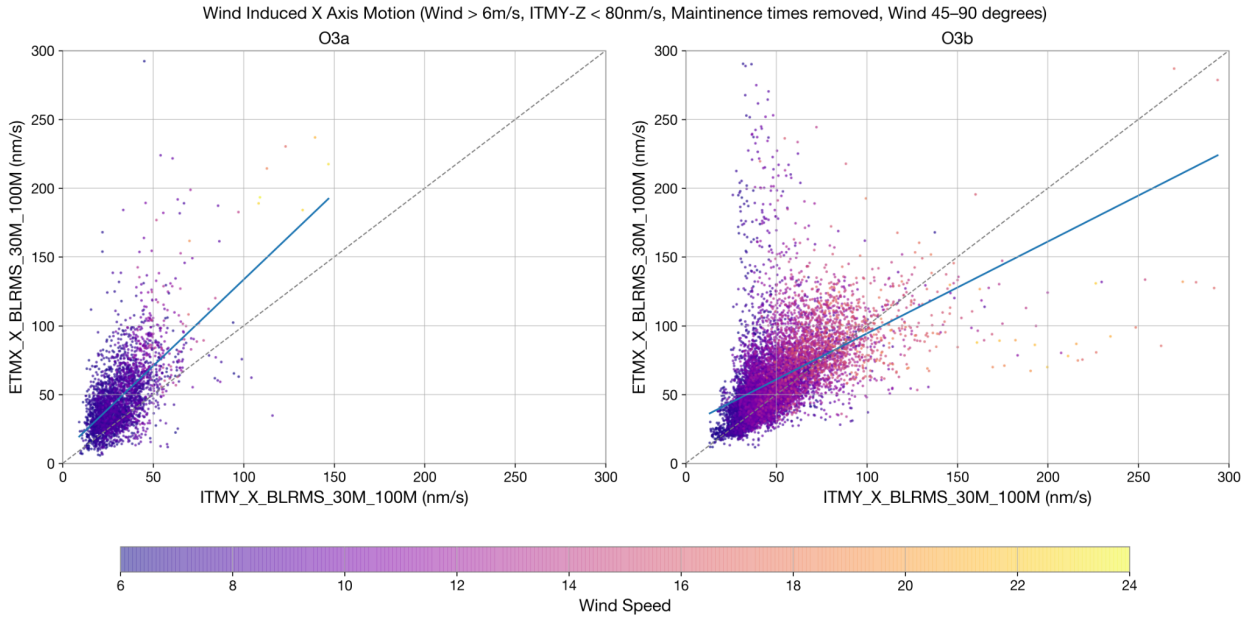

Figure 6.3: Relative performance of ITMY-X and EX STS-2 sensors for wind from 45º-90º during O3a and O3b. Lighter colored points indicate faster wind

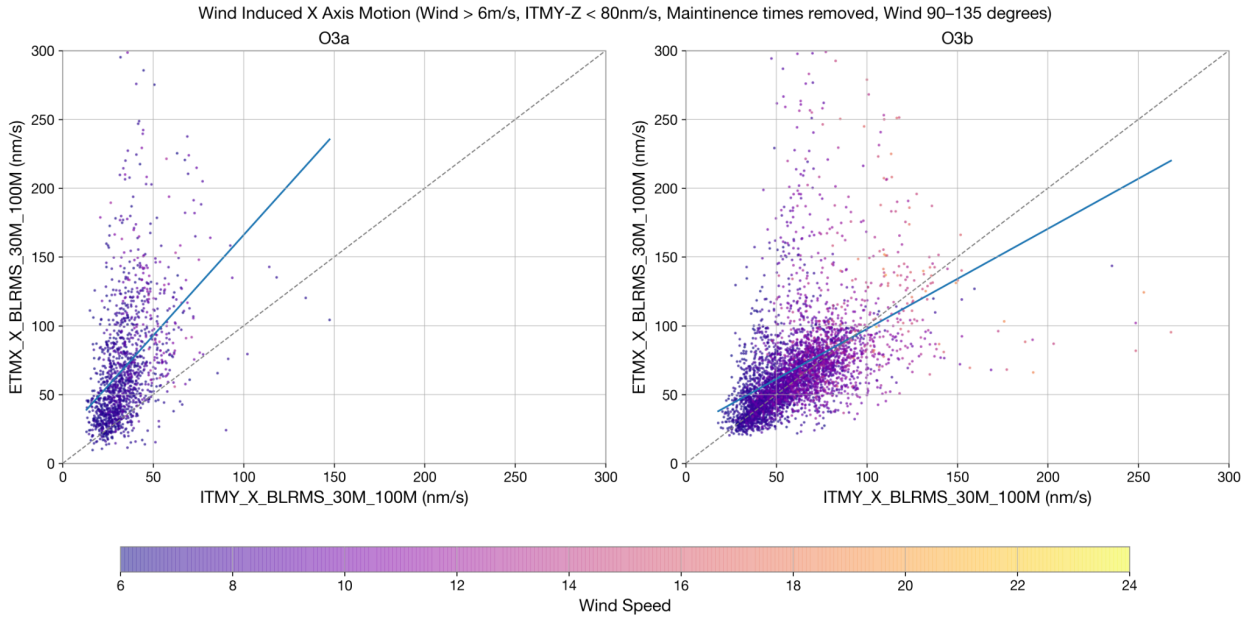

Figure 6.4: Relative performance of ITMY-X and End-X STS-2 sensors for wind from 90º-135º during O3a and O3b. Lighter colored points indicate faster wind

Figure 6.5 shows that for wind coming from directions which do not receive protection from the fence, we still see significantly more motion measured by the End-X STS-2 sensor.

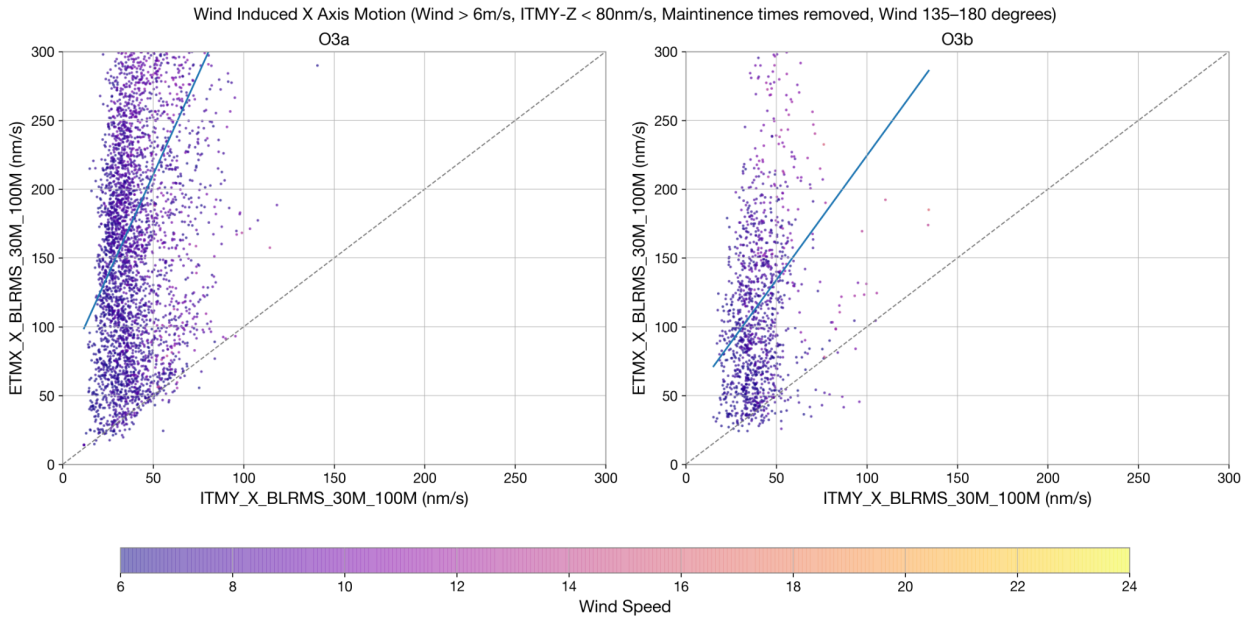

Figure 6.5: Relative performance of ITMY-X and End-X STS-2 sensors for wind from 135°-180° during O3a and O3b. Lighter colored points indicate faster wind

To further quantify the improvement from the fence we look at the improvement in EX STS-2 performance relative to ITMY-X performance (Fig. 6.6). Each point on this plot shows the average ratio of O3a EX:ITMY-X motion divided by the average ratio of O3b EX:ITMY-X motion for all time periods with wind greater than a particular value. For example, during O3a EX motion was on average 3.85 times greater than ITMY-X motion when wind speeds were >10 m/s, and during O3b EX motion was on average 1.22 times greater than ITMY-X motion when wind speeds were >10 m/s. Thus this correlates to the point (10 m/s, 3.16) on Figure 6.6. Looking at the figure we can clearly see that the fence is most effective for moderate wind between around 6-12 m/s, peaking at winds speeds of about 10 m/s. The spike in End-X performance improvement for wind speeds >15 m/s is likely due to a low sample size for these wind speeds skewing the results slightly.

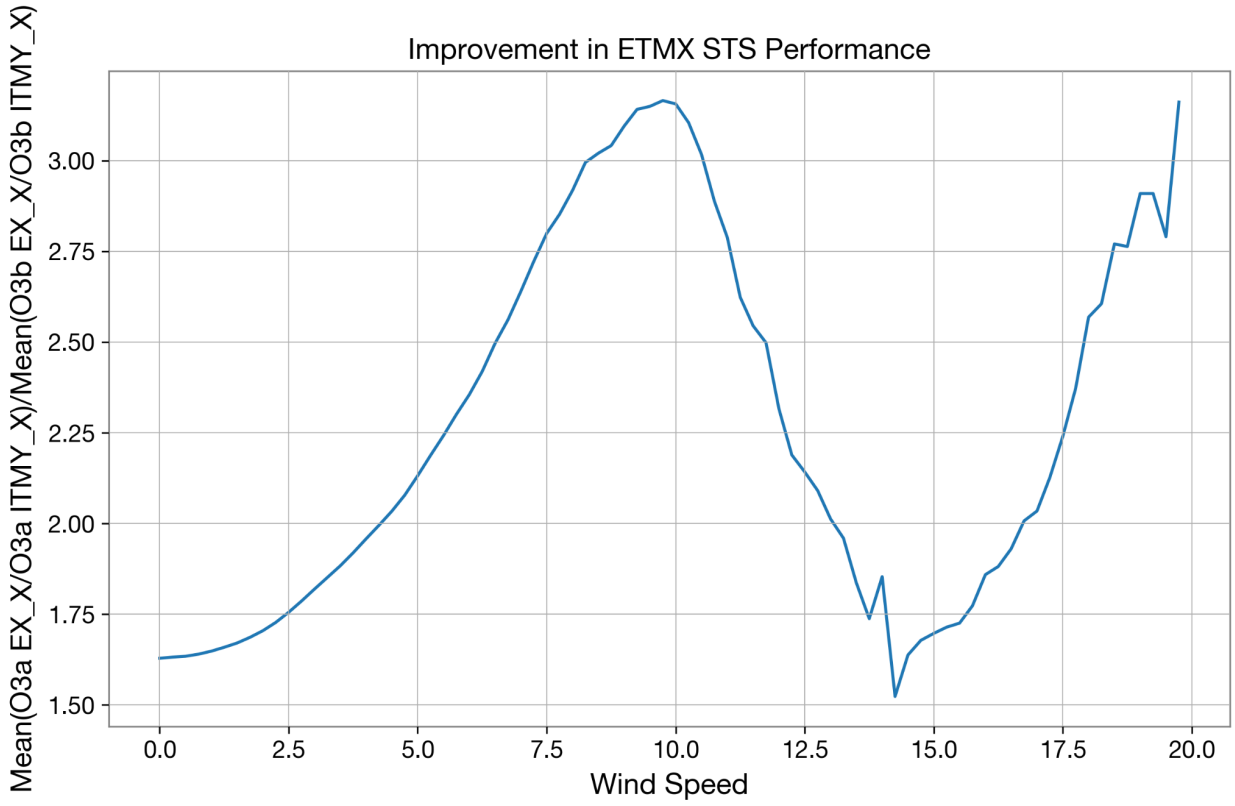

Figure 6.6: Relative improvement in EX STS-2 performance with respect to ITMY-X performance as a function of wind speed

6.1.2 30-100 mHz BLRMS STS-2 Motion at End-Y vs. ITMY

Looking at a similar plot comparing the End-Y STS-2 sensor to the ITMY sensor, we can see a similar albeit less dramatic trend. Figure 6.7 shows all minute long periods when the wind was faster than 6 m/s (as measured at the corner station) and the Z-axis motion was less than 80 nm/s. We see that although End-Y motion remains higher than ITMY-Y motion during O3b we can see that motion at End-Y has decreased significantly going from O3a to O3b, especially considering higher wind speeds.

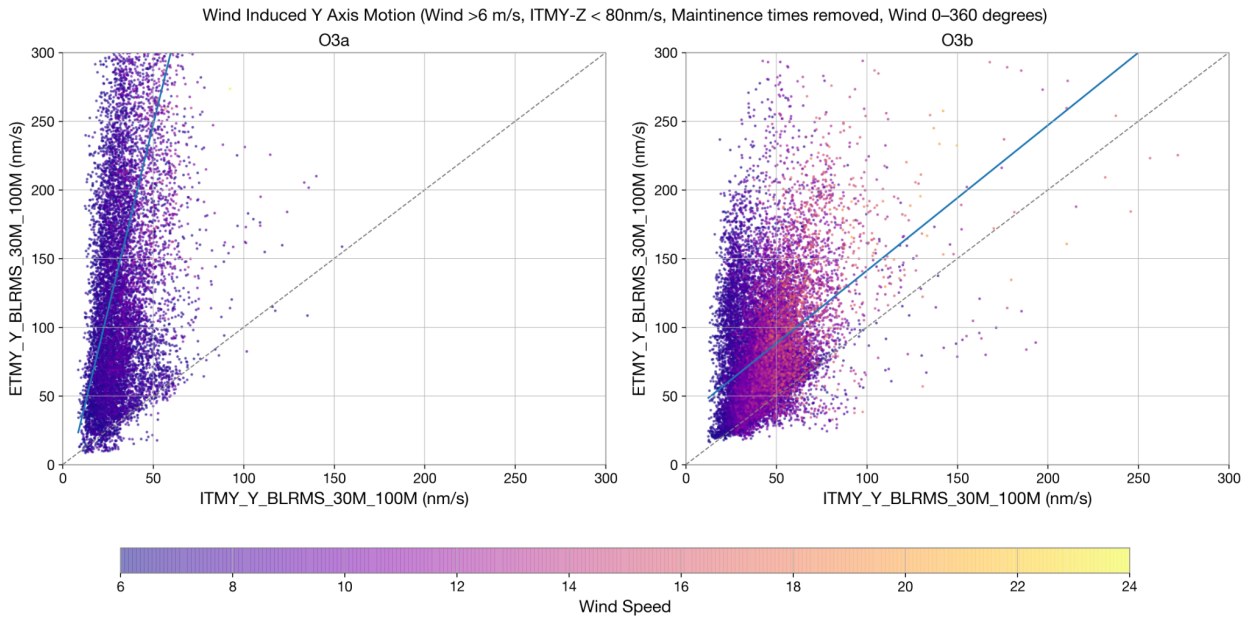

Figure 6.7: Relative performance of ITMY-Y and EY STS-2 sensors during O3a and O3b. Lighter colored points indicate faster wind

Disaggregating the data to show only desired wind direction we can once again see that the improvement that we see for winds coming from the protected direction (Fig. 6.8) dominates the overall trend of Figure 6.7, while other directions (Fig. 6.9) show some signs of reduced End-Y motion the effect is not nearly as pronounced and there is also not as much data for wind coming from those directions.

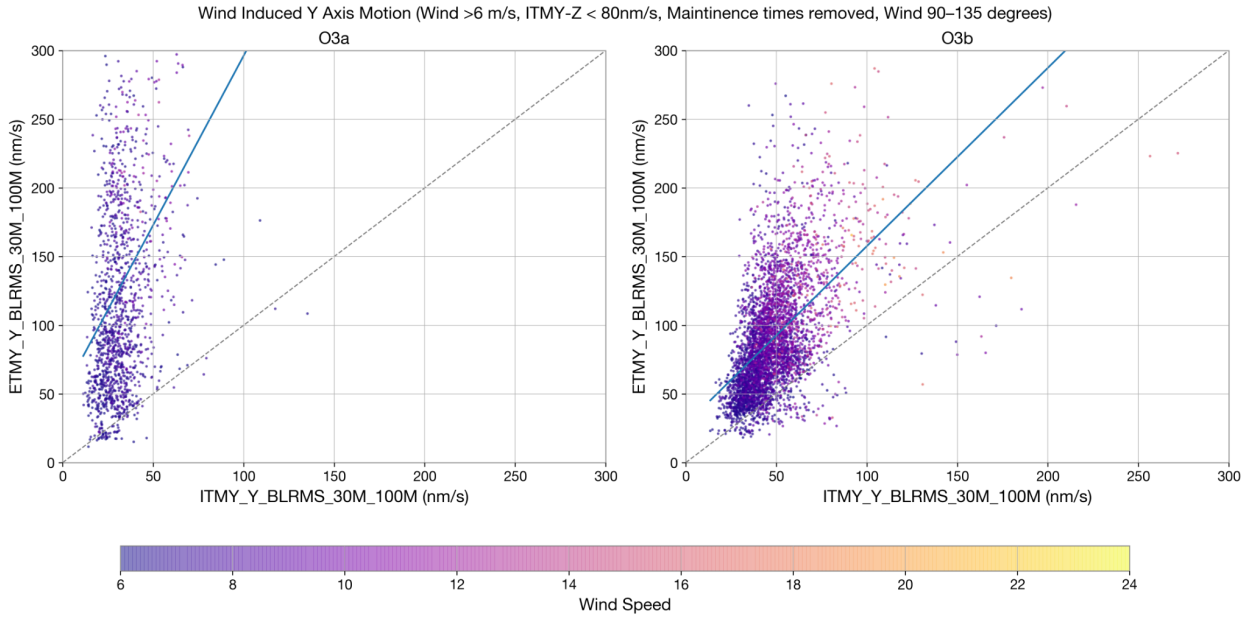

Figure 6.8: Relative performance of ITMY-Y and EY STS-2 sensors for wind from 90º-135º during O3a and O3b. Lighter colored points indicate faster wind

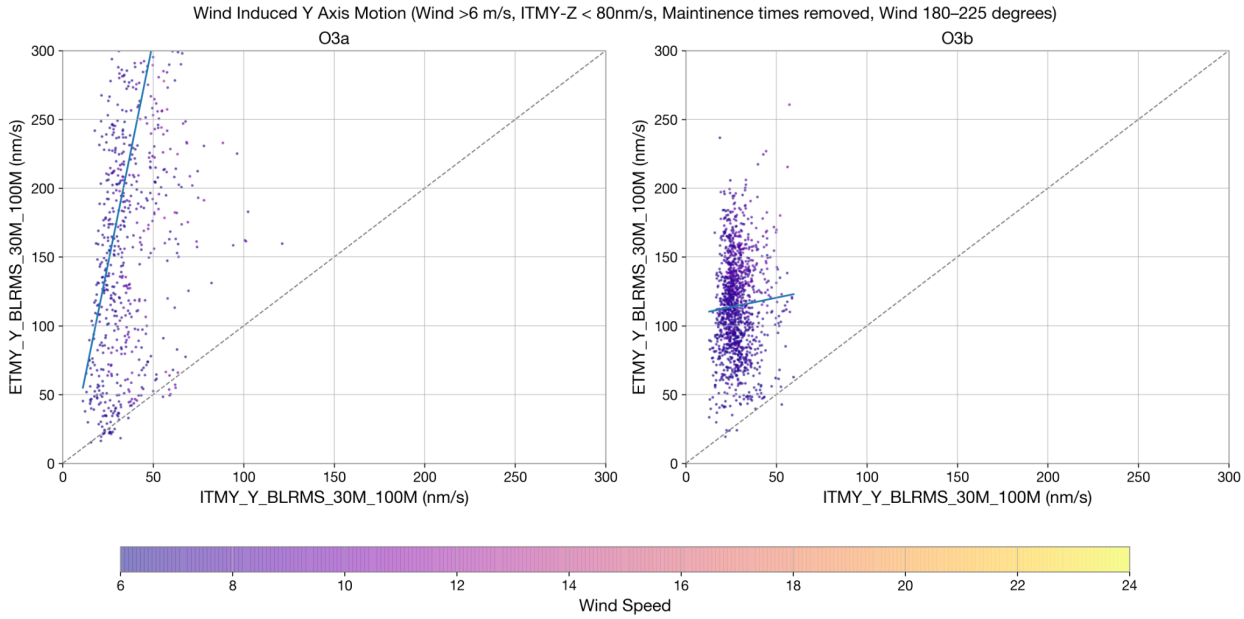

Figure 6.9: Relative performance of ITMY-Y and EY STS-2 sensors for wind from 90º-135º during O3a and O3b. Lighter colored points indicate faster wind

We can once again look at the relative improvement in End-Y performance as a function of wind speed. Figure 6.10 gives further evidence that the wind fences are most effective for moderate wind speeds with the most benefit begin observed for wind speeds of about 10 m/s.

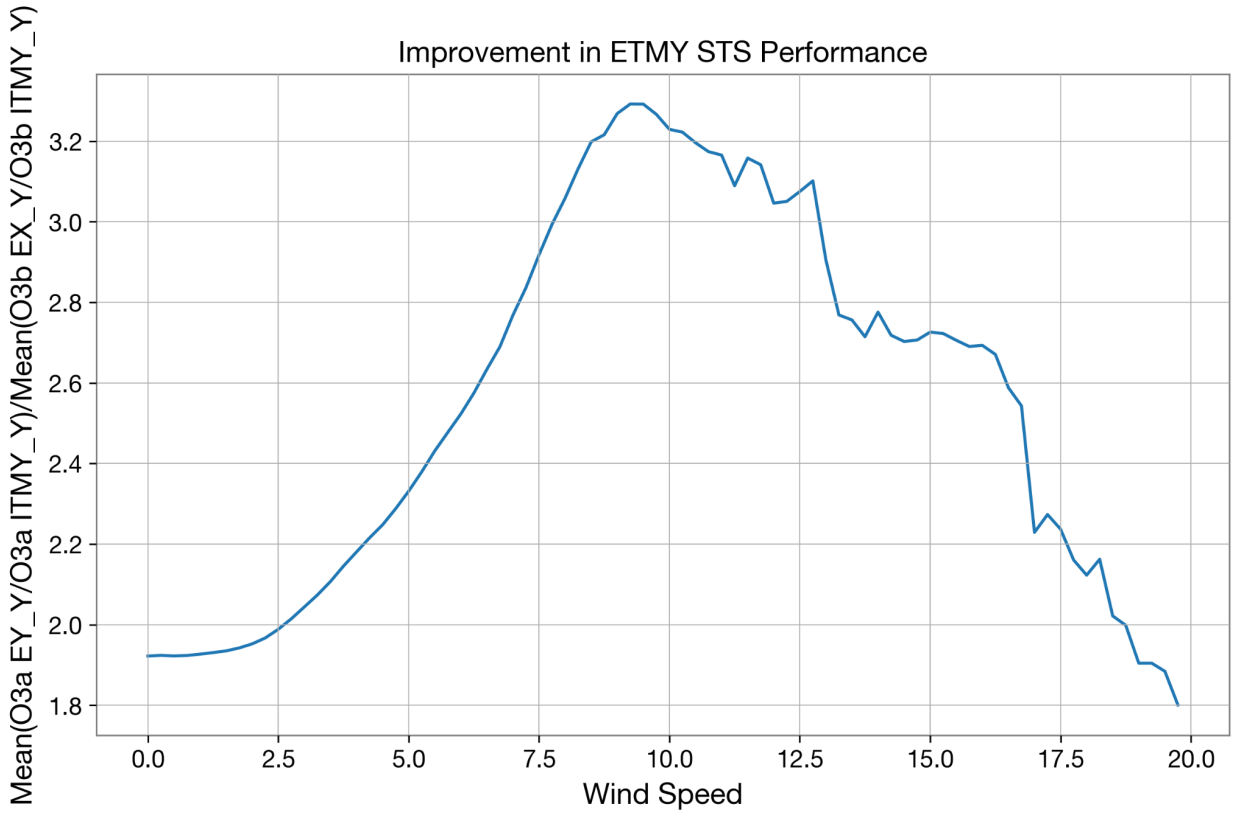

Figure 6.10: Relative improvement in EY STS-2 performance with respect to ITMY-Y performance as a function of wind speed

6.2 End Station Tilt-Subtracted STS-2 vs ITMY Motion

Although looking at the raw STS-2 data gives strong evidence for the efficacy of the wind fence, it does not tell the full story of the impact of wind on seismic isolation at the end vs the corner stations as the end stations are also equipped with BRS sensors designed to help subtract out the impact of tilt from the raw STS-2 signal. These tilt subtracted 30-100 mHz channels at the end stations are the primary channels used in LIGO's control systems. Comparing these channels gives us a sense of which observation station/which channel appears to be most impacted by high winds.

6.2.1 Tilt-Subtracted 30-100 mHz BLRMS STS-2 Motion at End-X vs. ITMY

Looking at all minute-long periods when the average wind speed was less than 6 m/s at the corner station and Z-axis 30-100 mHz BLRMS motion (Figure 6.11) we can see that even without the wind fence, the tilt subtracted End-X sensors tend to be less noisy than the ITMY sensor. The addition of the fence in O3b further improved the performance of the End-X sensors. Particularly notable are the very high wind speed periods (ie the lighter colors on the plot, wind speeds >~10 m/s), during which we see magnitude of End-X tilt subtracted motion being about 56.5% that of ITMY during O3b a significant reduction compared to the magnitude of End-X tilt subtracted motion being about 64.0% that of ITMY during O3b.

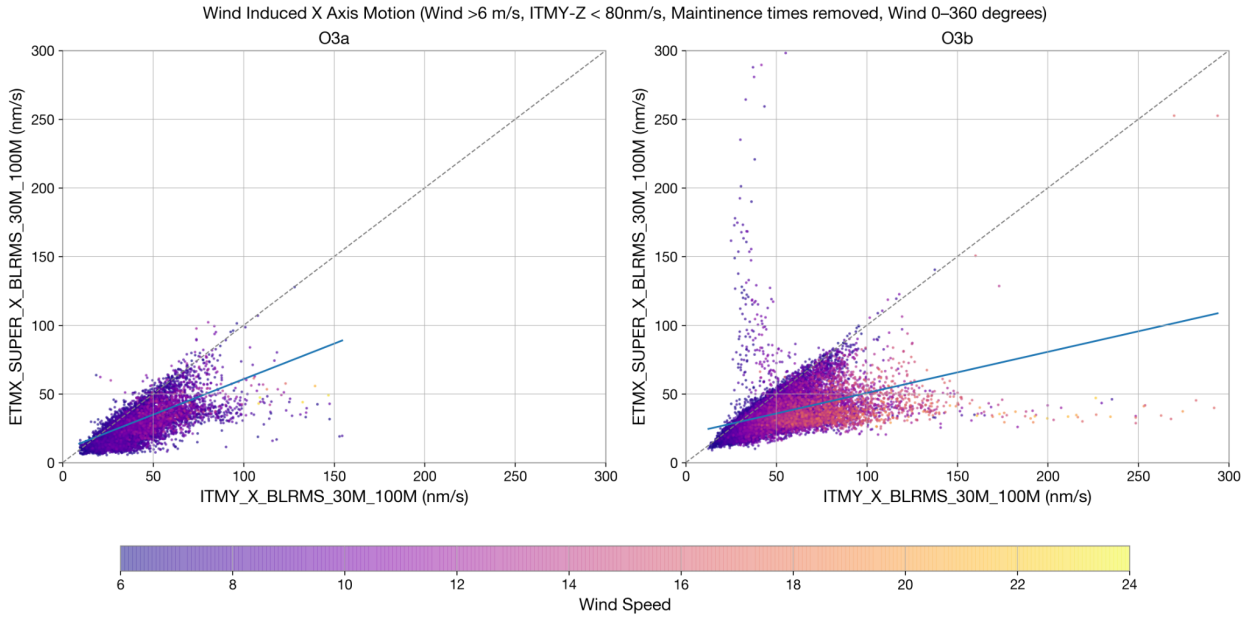

Figure 6.11: Relative performance of ITMY-X and tilt subtracted EX STS-2 sensors during O3a and O3b. Lighter colored points indicate faster wind

Once again, disaggregating this data by wind direction we can see the significant benefit derived from the wind fence for wind coming from protected directions (Fig. 6.12) as well as the lack of change when wind comes from unprotected directions (Fig. 6.13).

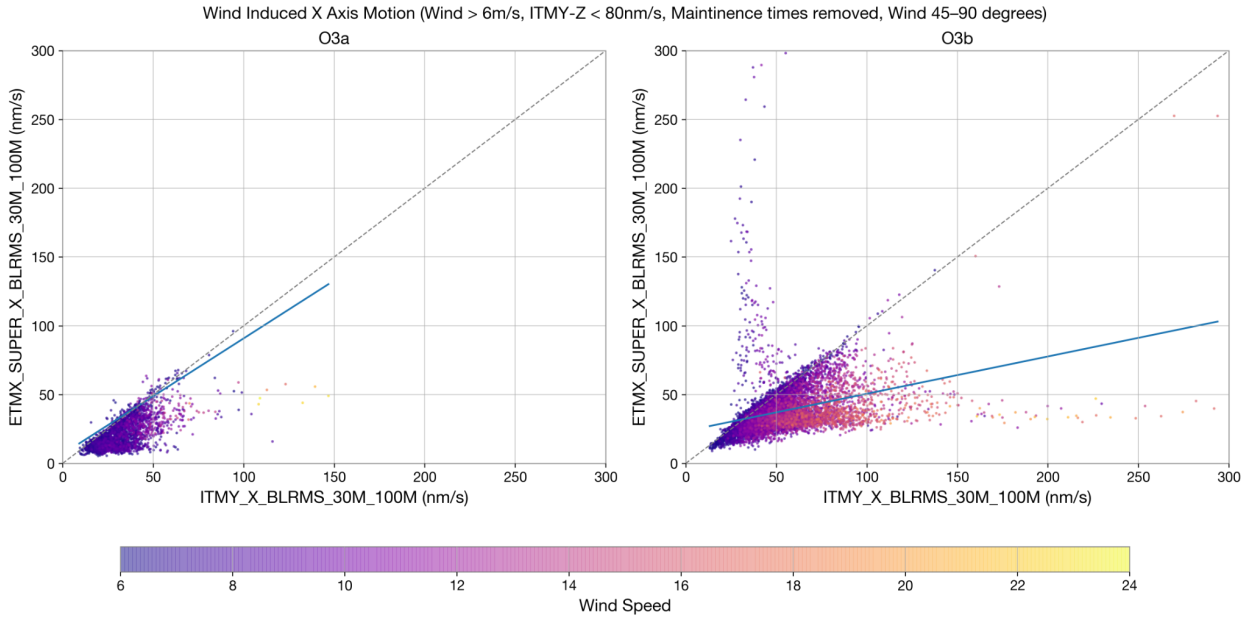

Figure 6.12: Relative performance of ITMY-X and tilt subtracted EX STS-2 sensors for wind from 45°-90° during O3a and O3b. Lighter colored points indicate faster wind

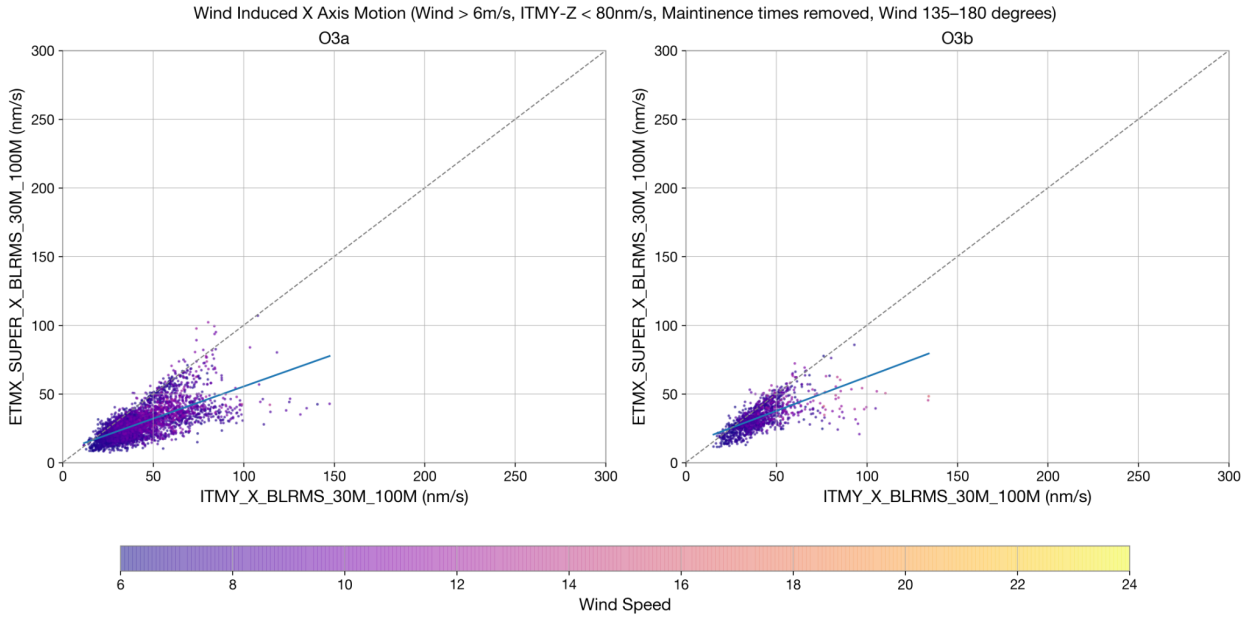

Figure 6.13: Relative performance of ITMY-X and tilt subtracted EX STS-2 sensors for wind from 135°-180° during O3a and O3b. Lighter colored points indicate faster wind

We can once again plot the relative improvement of tilt subtracted EX STS-2 performance (Fig 6.14). However here, we see much less apparent benefit derrivesd from the wind fence. This apparent lack of change is likely due to a combination of the fact that much of the effects of wind are already removed by the BRS for the tilt subsubtracted channel and the presence of excess ITMY-X motion during O3a which can be seen by examining the shape of the distributions in Figure 6.11.

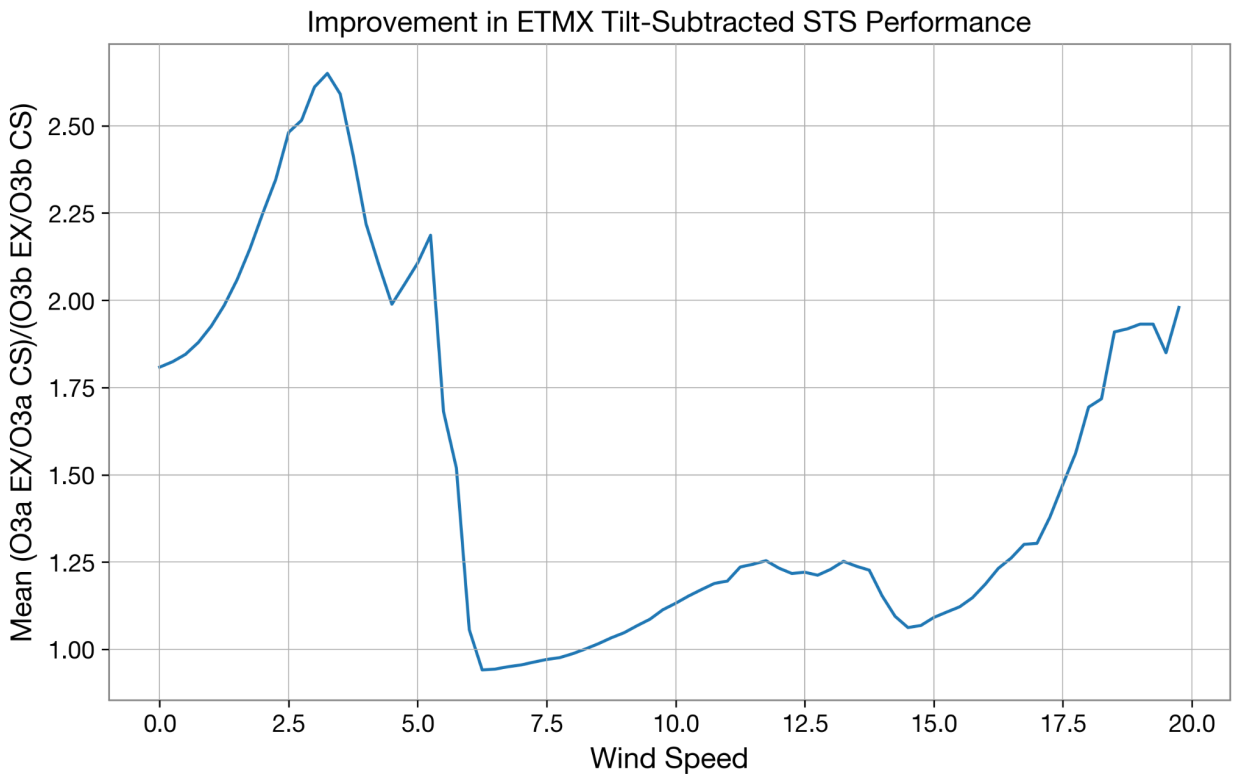

Figure 6.14: Relative improvement in tilt subtracted EX STS-2 performance with respect to ITMY-X performance as a function of wind speed

6.2.2 Tilt-Subtracted 30-100 mHz BLRMS STS-2 Motion at End-Y vs. ITMY

Creating the same plots for the End-Y tilt-subtracted STS-2 data, we once again observe a significant reduction in End-Y from O3a to O3b (Fig. 6.15). Notably, whereas the effects of the BRS tilt subtraction alone was not able to fully reduce end station motion to corner station levels, the effects of the BRS combined with the wind fence are actually able to reduce End-Y motion to the point where it now tends to be significantly less than the motion at the corner station.

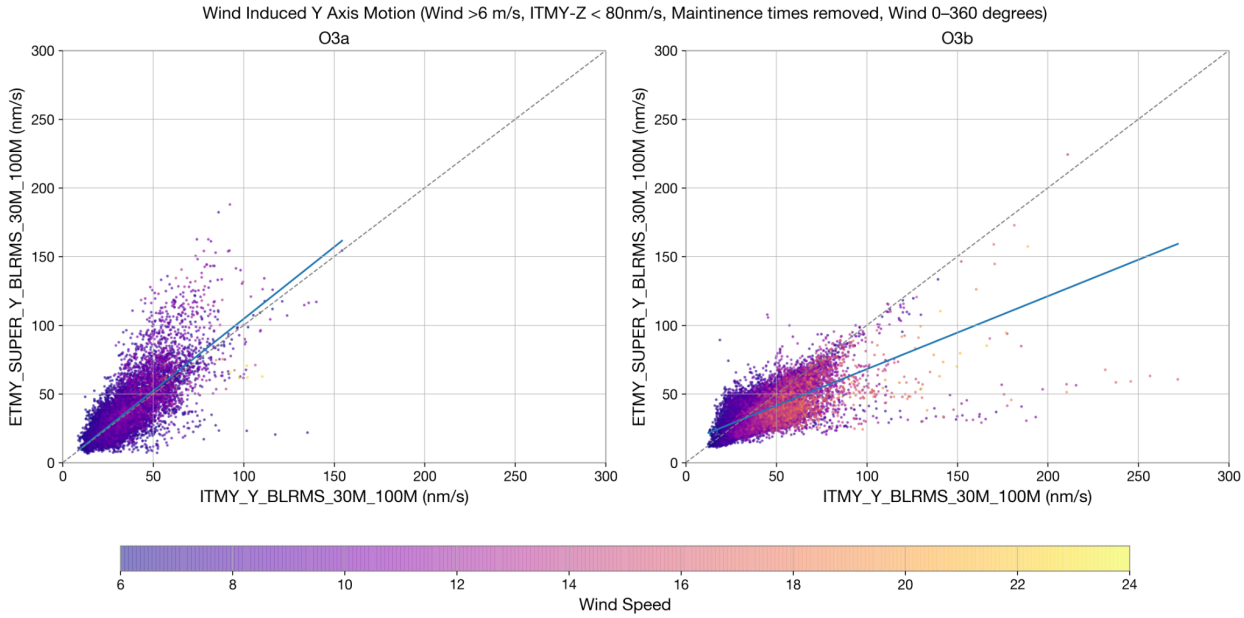

Figure 6.15: Relative performance of ITMY-Y and tilt subtracted EY STS-2 sensors during O3a and O3b. Lighter colored points indicate faster wind

Once again we can look as disaggregated data (Fig. 6.16 and 6.17) to verify that the fence is working in the expected directions (in this case the data do corroborate the findings from section 3 which show the End-Y fence functioning 45º-180º instead of the expected 45º-135º), and there is no significant change for the unprotected directions (Fig. 6.18).

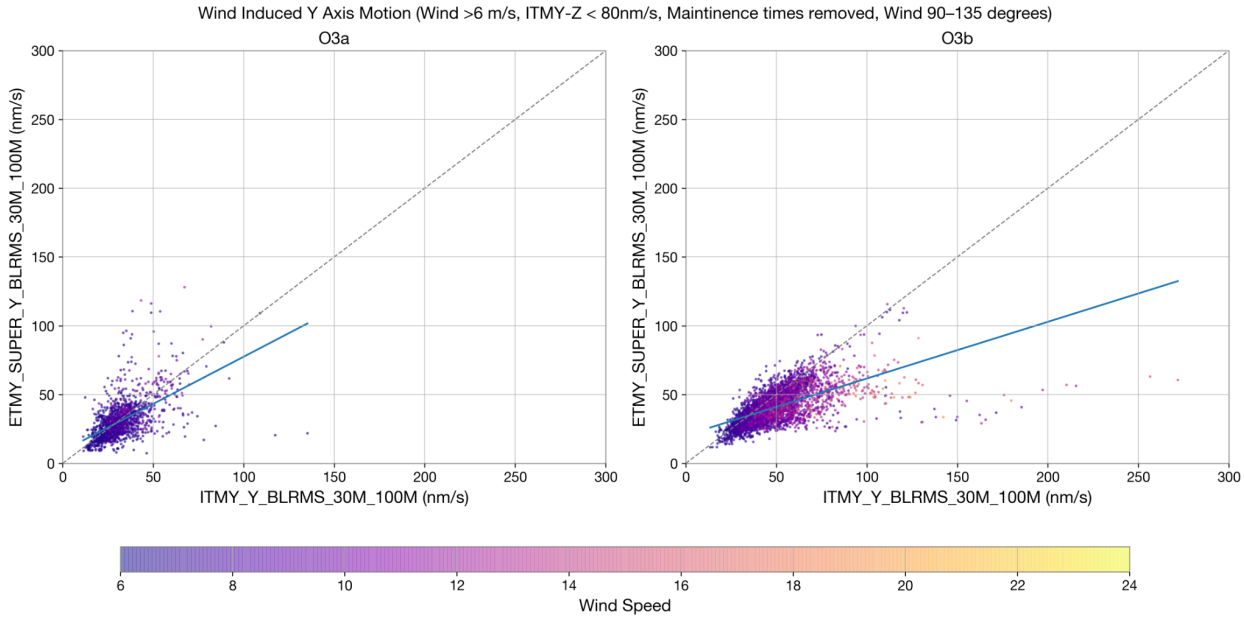

Figure 6.16: Relative performance of ITMY-Y and tilt subtracted EY STS-2 sensors for wind from 90º-135º during O3a and O3b. Lighter colored points indicate faster wind

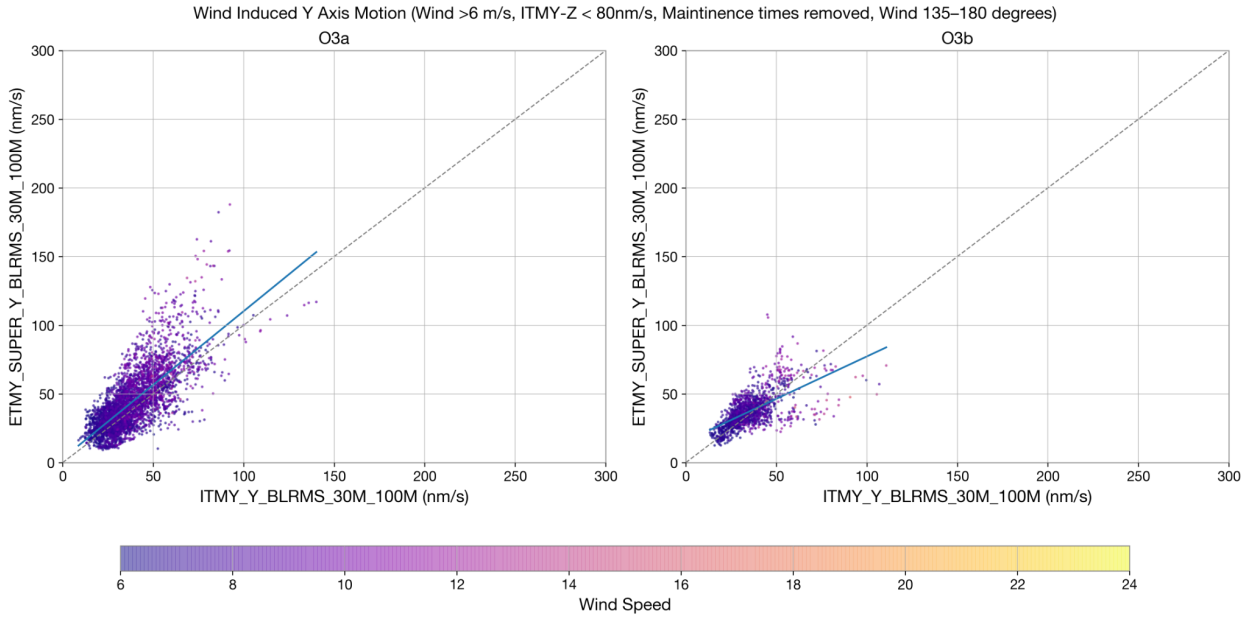

Figure 6.17: Relative performance of ITMY-Y and tilt subtracted EY STS-2 sensors for wind from 135°-180° during O3a and O3b. Lighter colored points indicate faster wind

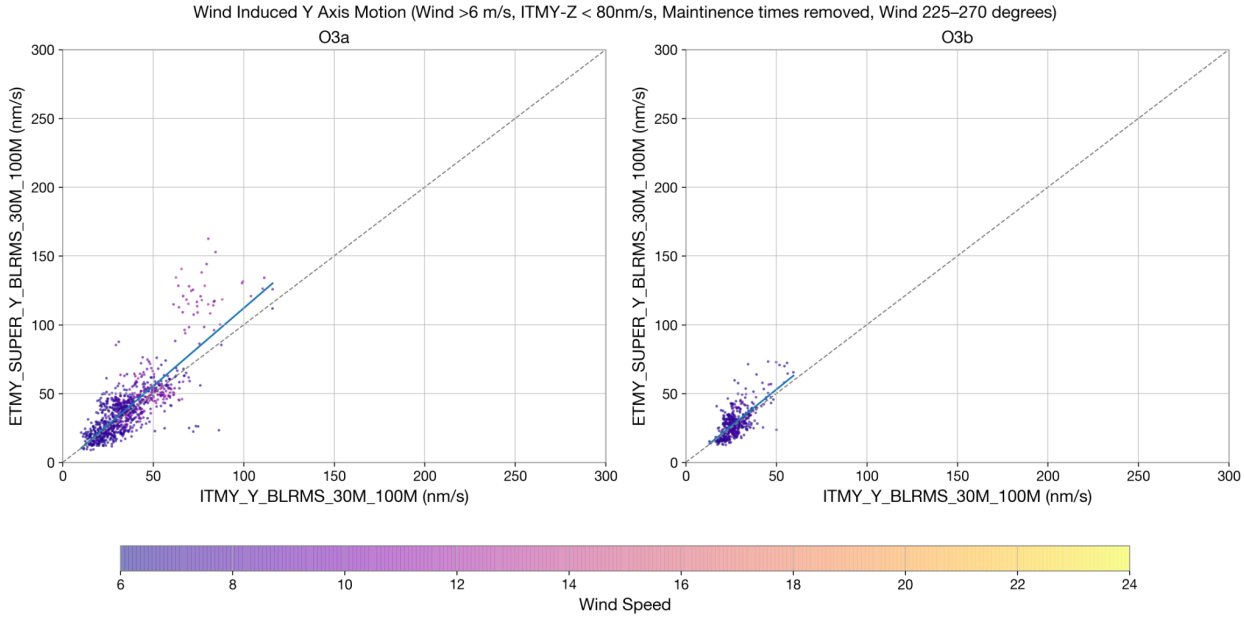

Figure 6.18: Relative performance of ITMY-Y and tilt subtracted EY STS-2 sensors for wind from 225°-270° during O3a and O3b. Lighter colored points indicate faster wind

7. Duty Cycle Analysis

Perhaps the most immediately obvious and easily interpretable way to evaluate the efficacy of the wind fences would be to simply compare the duty cycle as a function of wind speed during O3a and O3b. However, since duty cycle is influenced by many factors working in conjunction with each other and since many other improvements were made during the maintenance period, it is impossible to isolate the

effect of just the wind fence. That being said, looking at duty cycle is still useful for identifying major performance changes between O3a and O3b.

Figure 7.1 shows duty cycle as a function of wind speed for time periods when the ground motion (as measured by ITMY-Z) was under 80 nm/s during O3a and O3b. Markers are also used to indicate every 10th percentile of wind speed as well as the 95th 98th and 99th percentile for this specific range of data. This plot shows us that the duty cycle increased by 0.08-0.38 in O3b depending on the wind speed, with the most improvement coming for wind speeds between about 8-16 m/s.

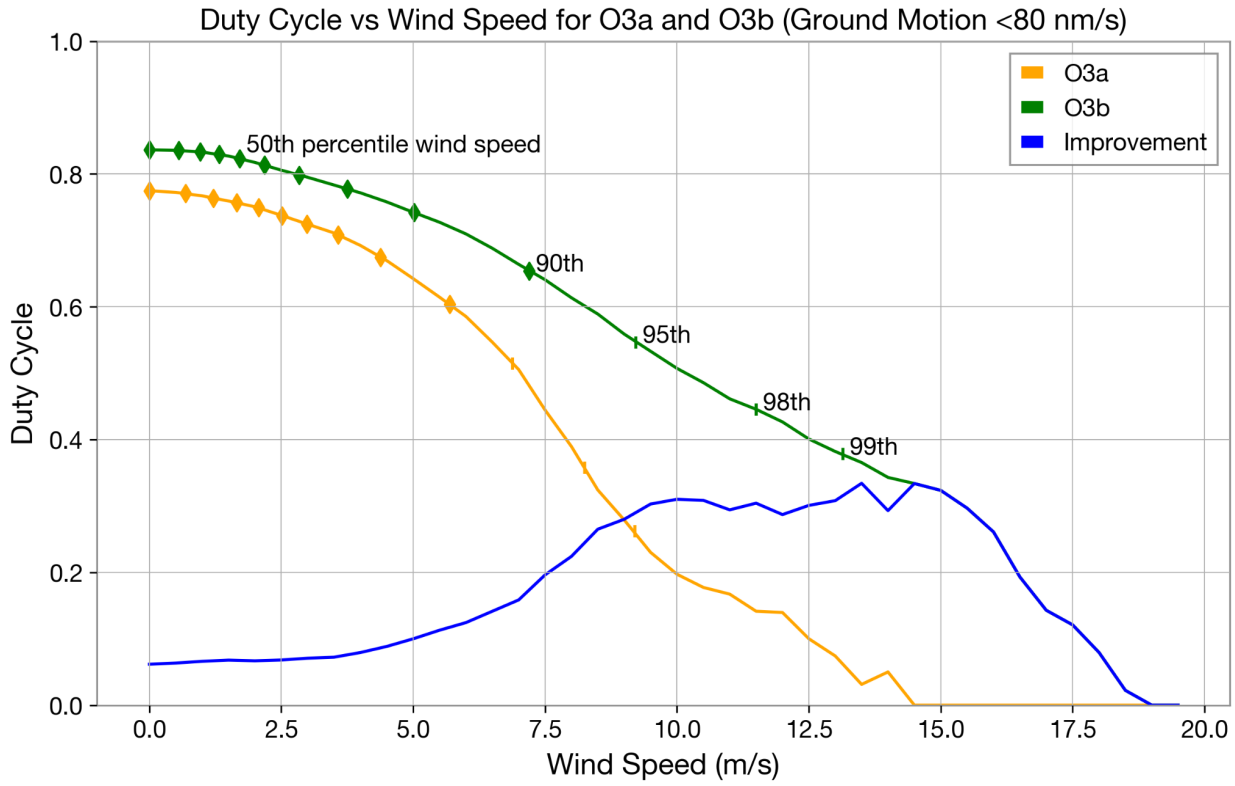

Figure 7.1: Duty cycle as a function of wind speed when ground motion <80 nm/s during O3a and O3b

To attempt to isolate the effects of just the wind fence we look at duty cycle as a function of wind speed for wind coming from each quadrant (centered on LIGOs axis) separately. Figure 7.2 shows that for times when wind came from the protected direction, there is an overall duty cycle improvement of about .05, this stays approximately constant until wind speeds of around 7.5 m/s at which point the improvement increases until reaching a maximum of around .4. However there is little data from O3a for wind speeds greater than 10 m/s which is where we see the most improvement which may impact the reliability of these results.

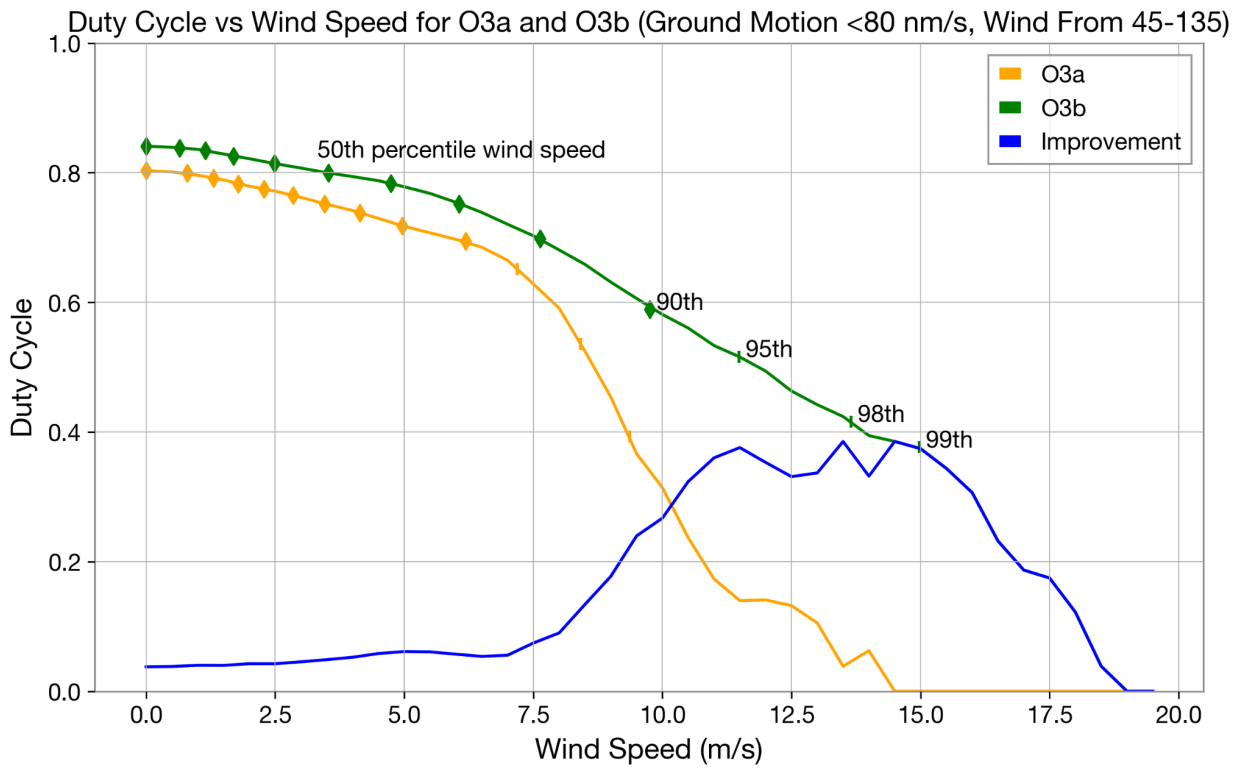

Figure 7.2: Duty cycle as a function of wind speed when ground motion <80 nm/s and wind from 45°-135° during O3a and O3b

Looking at wind from the +X (Fig 7.3) and the -Y (Fig 7.4) directions we actually see more improvement at lower wind speeds than we did for the +Y direction. Interestingly during O3b the speed of wind coming from the +X direction seemed to have no effect on the duty cycle until winds reached ~6 m/s at which point the duty cycle drops off rapidly. Similarly the speed of wind coming from the -Y direction seemed to have no noticeable effect on the duty cycle at all. It is possible that these results could just be due to wind from these directions largely being slow and unproblematic and there not being sufficient data for higher wind speeds. However, even if sample size for higher wind speeds were a problem we would still expect to see some reduction in duty cycle for medium speed winds around ~6 m/s for which we do have sufficient (ie multiple days worth) of data.

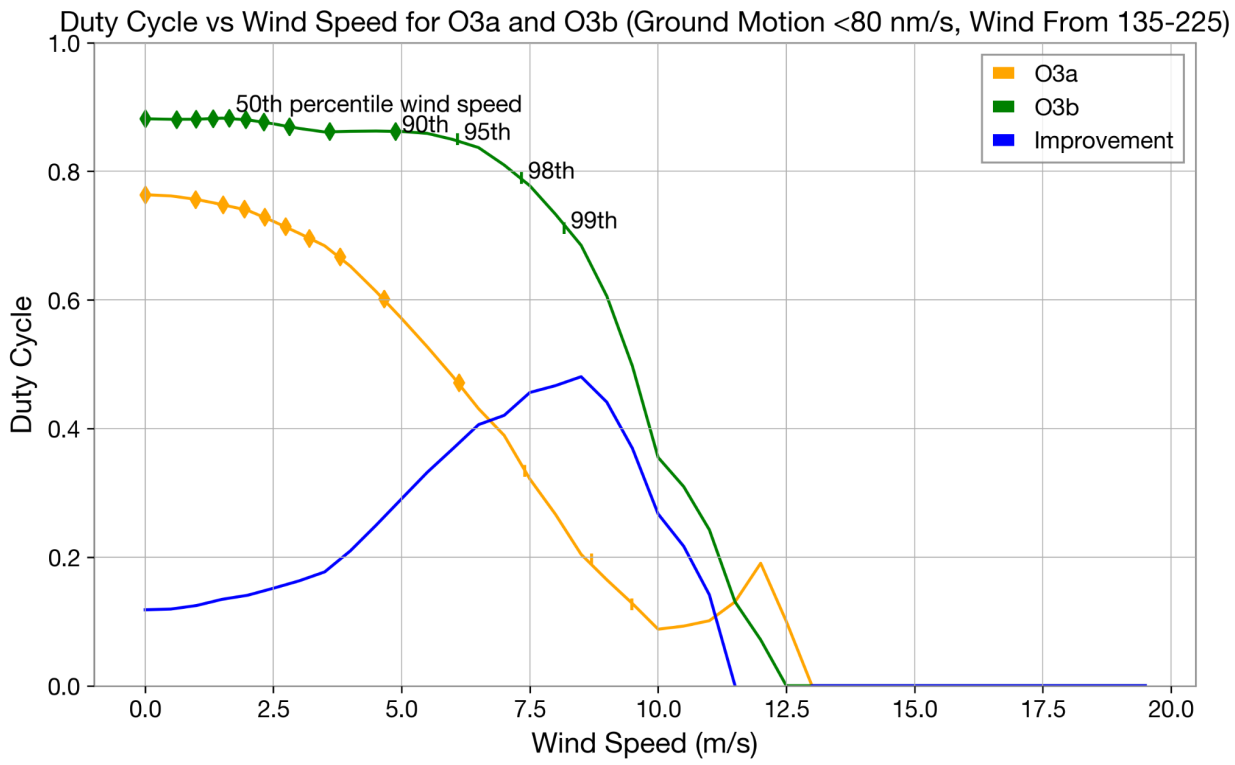

Figure 7.3: Duty cycle as a function of wind speed when ground motion <80 nm/s and wind from 135°-225° during O3a and O3b

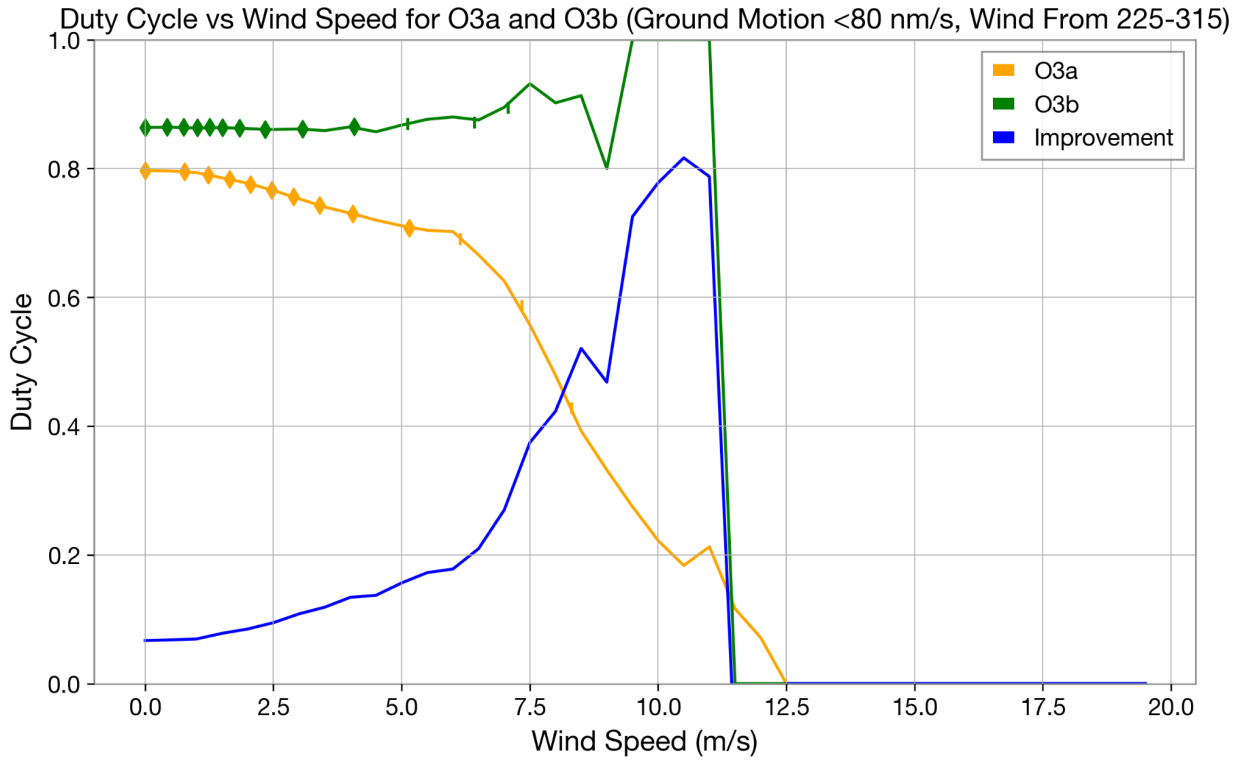

Figure 7.4: Duty cycle as a function of wind speed when ground motion <80 nm/s and wind from 225°-315° during O3a and O3b

Looking at the duty cycle for wind from the -X direction we see no significant difference between O3a and O3b. However the duty cycle for wind from this quadrant during O3a was greater than all other quadrants and more akin to performance for other wind directions during O3b.

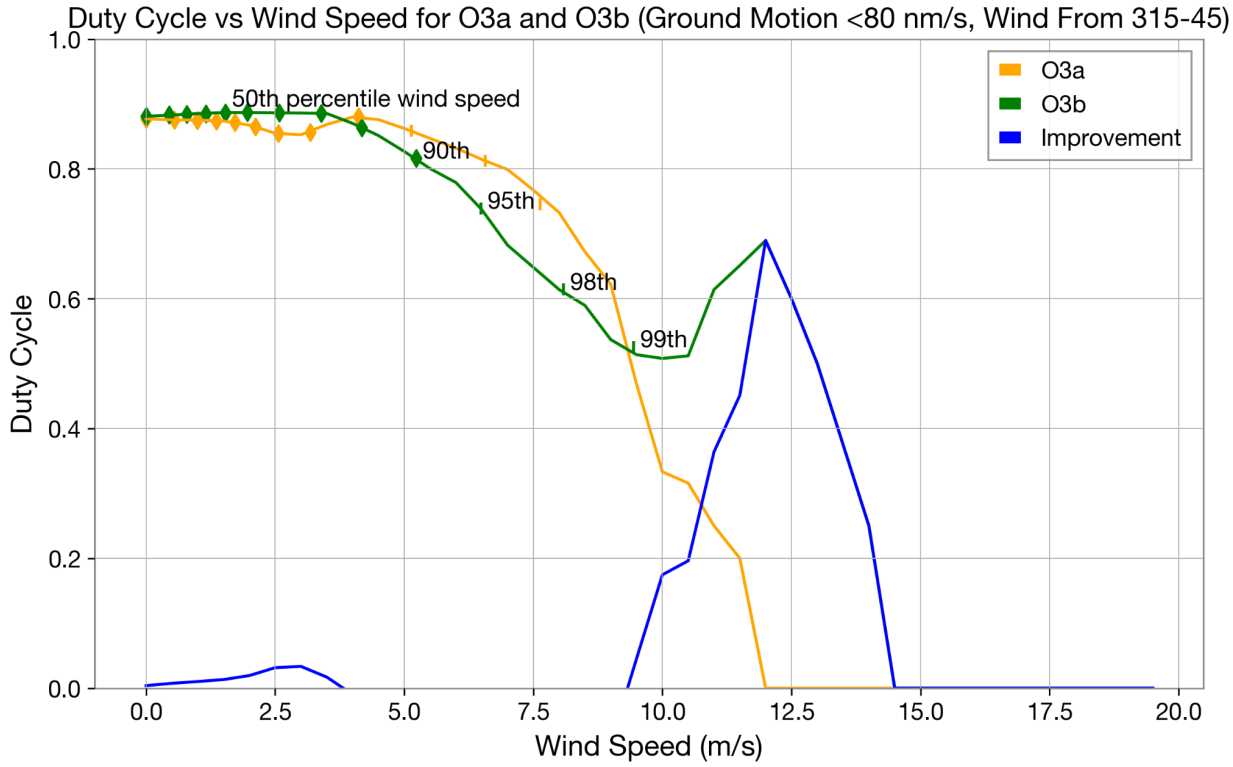

Figure 7.5: Duty cycle as a function of wind speed when ground motion <80 nm/s and wind from 315°-45° during O3a and O3b

Figure 7.6 overlays duty cycle plots for each of the four quadrants for O3a and O3b. Although O3b duty cycles were generally slightly better than O3a duty cycles, the similarities between the O3a -X trend line and the O3b (especially +X) trend lines are interesting to note. However, it is extremely difficult if not impossible to reach a complete understanding of all the factors affecting the duty cycle of the interferometer.

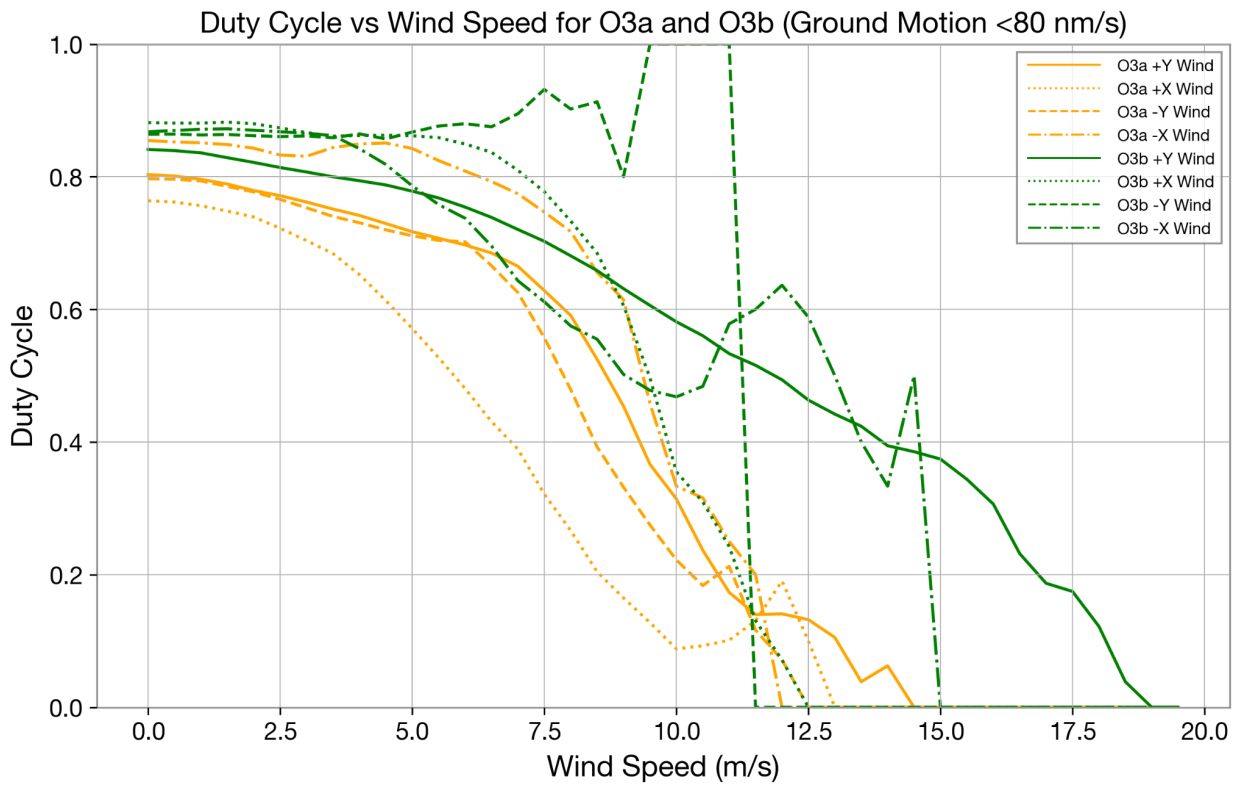

Figure 7.5: Duty cycle as a function of wind speed for each quadrant when ground motion <80 nm/s during O3a and O3b

8. Conclusion and Further Study

The main takeaway of these analyses is that the fence works well. More specifically we see that it has the potential to decrease the tilt by a factor of 3, additionally it has the potential to decrease the amount of floor motion measured at the end stations relative to the corner station by a factor of about 3. We see the maximal benefit of the fence for wind speeds around 10 m/s. Furthermore we can observe that the effects of the BRS tilt subtraction combined with the effects of the fence allow the end station's STS-2 sensors to be much less noisy than the ITMY sensor during high wind times, which may indicate that the next target of improvement should be windproofing the corner station. Another area of potential improvement may be to extend the fence to the north-west side of End-X since a significant amount of wind came from this direction unimpeded by the fence. This is in contrast to End-Y where the curvature of the fence does manage to slow wind blowing from the north-west.

The analysis of this paper raises a few questions as well. For one, End-Y still lacks a free stream wind sensor which is essential to be able to accurately and effectively evaluate the performance of the End-Y wind fence. Further instrumentation can also be useful to determine whether the fence reduces the turbulence of wind passing through it and whether or not this affects building tilts. This can also lead us to evaluate other things which affect building tilt and how, especially when the effects of wind should be negligible. Some deeper statistical analysis could yield insight into which observatory building is currently causing the most problems for glitches and the duty cycle when exposed to high wind, as well as into what the driving factors behind the duty cycle improvement between O3a and O3b were. For further study, drawing data from a longer period could be helpful. With the exception of the duty cycle section, no data used in this paper are affected by the operational status of the interferometer.

References

[ALOG39564] https://alog.ligo-wa.caltech.edu/aLOG/index.php?callRep=39564

[ALOG54680] https://alog.ligo-wa.caltech.edu/aLOG/index.php?callRep=54680

[GAO21] https://dcc.ligo.org/LIGO-T2100023

[HOF18] https://dcc.ligo.org/LIGO-G1801645

[HOF19] https://dcc.ligo.org/LIGO-T1900006/public

[LAN18] https://dcc.ligo.org/LIGO-G1800148

[VEN18] https://dcc.ligo.org/LIGO-P1800038-v4/public